GBE

Is Faster-X Adaptation Due to Large-Effect Mutations? An Empirical Test of a New Theory

Filip Ruzicka [1,*], Beatriz Vicoso [1]

[1]Institute of Science and Technology Austria, Klosterneuburg 3400, Austria

*Corresponding author: E-mail: ruzicka.filip@gmail.com.

Accepted: October 01, 2026

Abstract

A widespread observation in molecular evolution is that X-linked genes evolve faster—and often adapt faster—than autosomal genes. Three main ideas have been put forward to explain "faster-X" adaptation. The first is that new beneficial mutations are typically partially recessive with respect to fitness, leading to more efficient selection in hemizygous males. The second is that sex differences in recombination, or sex differences in variance in reproductive success, enhance the effective population size on the X chromosome relative to autosomes. Both ideas have limitations: the first conflicts with theories of dominance, in which beneficial mutations are proposed to be partially dominant, while the second only applies to some taxa. Here we tested a third, newly proposed theory, in which mutations with large "scaled phenotypic effects" (ie large effects relative to the distance to a phenotypic optimum) experience more positive selection on the X. Specifically, we used three proxies for scaled phenotypic effects—amino acid dissimilarity, amino acid conservation, and gene age—and estimated X and autosomal rates of adaptation of nonsynonymous mutations across effect-size classes. We did this in three lineages with a well-documented faster-X: *Drosophila melanogaster*, *Mus musculus*, and *Homo sapiens*. As expected, we found that large-effect mutations were more likely to be under purifying selection and less likely to be under positive selection than small-effect mutations. However, contrary to the new theory, faster-X adaptation was not enriched among large-effect mutations. Overall, our results highlight an unresolved gap between patterns of sex chromosome evolution and theories of dominance for fitness.

Key words: evolutionary biology, population genetics, sex chromosomes, adaptation, genetic divergence, McDonald–Kreitman test, Fisher's geometric model.

Significance

In many species, genes on the X chromosome undergo more adaptation than autosomal genes, but it is not clear why this pattern of "faster-X" occurs. One possibility is that recessive beneficial mutations drive the effect, but theories of dominance propose instead that beneficial mutations should be dominant. Meanwhile, alternative explanations (eg sex differences in recombination or sex differences in variance in reproductive success) only apply to some taxa. Here we tested a new idea, in which the effect is driven by mutations with large effects. However, data from fruit flies, humans, and mice did not support the new theory. Our work highlights an unresolved gap between patterns of sex chromosome evolution and theories of dominance for fitness.

© The Author(s) 2026. Published by Oxford University Press on behalf of Society for Molecular Biology and Evolution.
This is an Open Access article distributed under the terms of the Creative Commons Attribution-NonCommercial License (https://creativecommons.org/licenses/by-nc/4.0/), which permits non-commercial re-use, distribution, and reproduction in any medium, provided the original work is properly cited. For commercial re-use, please contact reprints@oup.com for reprints and translation rights for reprints. All other permissions can be obtained through our RightsLink service via the Permissions link on the article page on our site—for further information please contact journals.permissions@oup.com.

Downloaded from academic.oup.com/gbe/article/18/10/evag259/8907347 by library@ist.ac.at user on 23 October 2026

Introduction

Empirical tests of evolutionary theories require exceptional study systems in which model parameters are both measurable and allowed to vary. In species with genetic sex determination, X-linked and autosomal genes exhibit different modes of inheritance, generating fortuitous natural variation in many genetic parameters and permitting a wide range of inferences about evolution (Vicoso and Charlesworth 2006; Ellegren 2009; Wilson Sayres 2018). For example, X-autosome contrasts have been used to estimate sex differences in mutation rates (Miyata et al. 1987; Wilson Sayres and Makova 2011; Connallon et al. 2022), breeding ratios (Hammer et al. 2010; Lohmueller et al. 2010), and migration rates (Juric et al. 2016; Goldberg et al. 2017; Osada et al. 2020; Chevy et al. 2023). X-autosome contrasts have also been used to infer the dominance coefficients of deleterious mutations (Avery 1984; Mallet et al. 2011; Veeramah et al. 2014; Ruzicka et al. 2021), beneficial mutations (Haldane 1927; Charlesworth et al. 1987, 2018; Orr 2010; Veeramah et al. 2014), and sexually antagonistic mutations (Rice 1984; Fry 2010; Frank and Patten 2020; Ruzicka and Connallon 2020, 2022). And they are key components of hypotheses about genome evolution (Meisel et al. 2009; Vibranovski et al. 2009; Toups and Hahn 2010), lifespan (Brengdahl et al. 2018; Sultanova et al. 2018, 2023; Connallon et al. 2022) and speciation (Turelli and Orr 1995, 2000; Masly and Presgraves 2007; Ellegren et al. 2012; Sankararaman et al. 2016; Presgraves 2018).

In the last 20 years, a consistent pattern has emerged from X-autosome comparisons (Meisel and Connallon 2013; Charlesworth et al. 2018; McDonough et al. 2024): namely, that functional sequence divergence is elevated among X-linked genes, relative to autosomal genes (Baines et al. 2008; Vicoso et al. 2013; Sackton et al. 2014; Wright et al. 2015; Jaquiéry et al. 2018; Bechsgaard et al. 2019; Mongue et al. 2022; Darolti et al. 2023; Mongue and Baird 2024). This pattern of "faster-X (or faster-Z) evolution" can either be driven by less effective purifying selection (ie selection favoring the removal of deleterious mutations), or more effective positive selection (ie selection favoring the fixation of beneficial mutations), on the X chromosome relative to autosomes (Vicoso and Charlesworth 2009; Mank et al. 2010). In some cases, the contributions of positive selection to faster-X evolution have been isolated, using McDonald–Kreitman (MK) tests that compare polymorphism and divergence (McDonald and Kreitman 1991; Eyre-Walker and Keightley 2009; Galtier 2016), or population genomic signals of selective sweeps. A pattern of "faster-X (or faster-Z) adaptation" often emerges (see McDonough et al. 2024 for a recent review), as in the case of *Heliconius* butterflies (Pinharanda et al. 2019), *Drosophila* fruit flies (Ávila et al. 2014; Campos et al. 2014; Garrigan et al. 2014; Harris et al. 2024), apes (Hvilsom et al. 2012; Veeramah et al. 2014; Dutheil et al. 2015), and rodents (Carneiro et al. 2012; Kousathanas et al. 2014). Some species, often ZW systems, show no significant X/Z-autosome differences (Rousselle et al. 2016; Hayes et al. 2020; Baird et al. 2025; Chase et al. 2025), though the only clear example of faster-autosome adaptation to date is the blood fluke *Schistosoma japonicum*, in which Z-linked effective population sizes (N_e) are drastically reduced (Mrnjavac and Vicoso 2025). Moreover, an analogous pattern of "faster-haploid" adaptation, relative to diploids, has been repeatedly reported in experimental populations of the budding yeast *Saccharomyces cerevisiae* (Zeyl et al. 2003; Gerstein et al. 2011; Marad et al. 2018).

Three main ideas have been put forward to explain faster-X *adaptation*. The first and most commonly invoked idea is that beneficial mutations are on average partially recessive with respect to fitness (Charlesworth et al. 1987; Orr and Otto 1994). Partially recessive beneficial mutations that arise on the X are immediately exposed to positive selection in hemizygous (haploid) males, which—assuming adaptation proceeds from new mutations, equivalent fitness effects of homozygotes and hemizygotes, and $N_{eX} = ¾\ N_{eA}$—enhances their substitution rates relative to equivalent autosomal mutations (Avery 1984; Charlesworth et al. 1987). This faster-X prediction when beneficial mutations are recessive is further exacerbated when selection is stronger in males than in females (Charlesworth et al. 1987; Meisel and Connallon 2013). This hypothesis is appealing because the dominance of mutations might be relatively similar across taxa, thus providing a general explanation for faster-X adaptation. However, the hypothesis also conflicts with theories of dominance for fitness, which propose that new beneficial mutations are on average partially dominant and/or overdominant for fitness (Manna et al. 2011; Sellis et al. 2011; McDonough and Connallon 2023). If theories of dominance are correct, faster-autosome adaptation is to be expected, since autosomes reap the benefits of elevated mutational input while suffering minimal reductions in fixation probability due to incomplete dominance (Charlesworth et al. 1987; Meisel and Connallon 2013). Theories of dominance for fitness are widely supported by the observation that spontaneous deleterious mutations, especially strongly deleterious ones (Charlesworth 1979; Orr 1991; Agrawal and Whitlock 2011), are partially recessive (Manna et al. 2011). Direct data on the dominance of beneficial mutations are much sparser, and

Downloaded from academic.oup.com/gbe/article/18/10/evag259/8907347 by library@ist.ac.at user on 23 October 2026

often biased by differences in fixation probability of dominant vs. recessive mutations (ie "Haldane's sieve"), resulting in highly variable estimates (Bourguet and Raymond 1998; Anderson et al. 2004; Gerstein et al. 2011, 2014; Ronfort and Glémin 2013; Sellis et al. 2016; Marad et al. 2018; Aggeli et al. 2022).

A second idea is that sex differences in variance in reproductive success, or sex differences in recombination rate, generate conditions where $N_{eX} > ¾\ N_{eA}$. For example, high variances in reproductive success tend to reduce N_e (Charlesworth 2009), and such reductions are weaker on the X when variance in reproductive success is higher in males than females (Charlesworth 2001; Vicoso and Charlesworth 2009), due to the X chromosome's female-biased transmission. Similarly, Hill–Robertson interference between mutations can be modeled as a reduction in N_e (Charlesworth 2009), and this reduction is weaker on the X in species where male recombination is less frequent than female recombination (Charlesworth et al. 2018), again because of the X chromosome's female-biased transmission. Thus, sex differences in variance in reproductive success or recombination rate can elevate N_{eX}/N_{eA}, potentially favoring faster-X adaptation even when beneficial mutations are partially dominant (Vicoso and Charlesworth 2009; Charlesworth et al. 2018). For example, the total absence of recombination in males of *Drosophila melanogaster* elevates X-autosome ratios of neutral diversity above 1 in some populations of this species (Charlesworth et al. 2018), which has been shown to contribute to faster-X adaptation (Campos et al. 2014). However, faster-X is also observed in *D. melanogaster* among pairs of genes with similar "effective" (sex-linkage-adjusted) recombination rates on the X and autosomes (Campos et al. 2013, 2014; Charlesworth et al. 2018). Moreover, signals of faster-X adaptation are found in species where X-autosome ratios of neutral diversity are near or below ¾ (Leffler et al. 2012), such as humans (Veeramah et al. 2014) and house mice (Kousathanas et al. 2014), which requires a different explanation.

Recently, a third idea to explain faster-X adaptation has been proposed (McDonough et al. 2024), in which mutations with large "scaled phenotypic effects" (ie large phenotypic effects relative to the distance to a phenotypic optimum) generate more positive selection on the X. As in classical faster-X theory, McDonough et al.'s (2024) theory assumes that adaptation proceeds by the sequential fixation of new mutations and that X-linked genes lack a functional Y-linked homolog. However, they explicitly model the fitness effects of mutations using Fisher's geometric model, such that new mutations pleiotropically affect many traits under stabilizing selection toward a single phenotypic optimum. The rationale for faster-X adaptation is then as follows: (i) mutations can have large scaled phenotypic effects (ie either because phenotypic effects are large in absolute terms, or the optimum is nearby; see left vs. right panels of Fig. 1a) (Orr 1998); (ii) large-effect mutations will typically undergo purifying selection (gray dots in Fig. 1a)—intuitively, this is because random mutations are much more likely to break than to improve a complex system (Fisher 1930; Waxman and Welch 2005)—but they can sometimes exhibit overdominance for fitness (red and yellow dots in Fig. 1a) (Sellis et al. 2011; McDonough and Connallon 2023; Ruzicka et al. 2026); (iii) overdominant mutations are subject to balancing selection and should remain polymorphic on autosomes, whereas the same mutations on the X chromosome can experience positive selection and rapidly become fixed (yellow dots in Fig. 1a) (Pamilo 1979). In other words, the model proposes that X-linkage converts a subset of mutations from evolving under balancing selection to evolving under positive selection (Fig. 1a), thereby generating an excess of adaptive substitutions on the X. A simple prediction of the model is that large-effect mutations should exhibit relatively high X-autosome ratios of rates of adaptive substitution compared to small-effect mutations because large-effect mutations are more susceptible to this "conversion" of balancing selection to positive selection on the X (Fig. 1b and c). McDonough et al.'s (2024) idea is appealing because it is consistent with leading theories of dominance (Manna et al. 2011), though it may still fail to generate faster-X if (for example) scaled phenotypic effects are consistently too small in real populations, or if scaled phenotypic effects cannot be accurately inferred.

Here, we tested McDonough et al.'s (2024) new hypothesis for faster-X adaptation by comparing X-autosome ratios of adaptive substitution rates, inferred from MK tests, among mutations of different effect sizes. Specifically, we used three proxies for the scaled phenotypic effects of mutations: differences in the physico-chemical properties of amino acid pairs (Grantham 1974; Bergman and Eyre-Walker 2019)—which are intended to capture variation in the absolute phenotypic effect of mutations (right panel of Fig. 1a)—and differences in amino acid conservation (Vaser et al. 2016; Chen et al. 2022) and gene age (Domazet-Lošo et al. 2017; Moutinho et al. 2022)—which are intended to capture variation in the distance to the phenotypic optimum (left panel of Fig. 1a). We then examined whether signals of faster-X adaptation are stronger among large-effect than small-effect mutations. We applied this test to three model organisms covering a range of N_{eX}/N_{eA} ratios—above 1 in the fruit fly (*D. melanogaster*) (Ávila et al. 2014; Campos et al. 2014), below

Downloaded from academic.oup.com/gbe/article/18/10/evag259/8907347 by library@ist.ac.at user on 23 October 2026

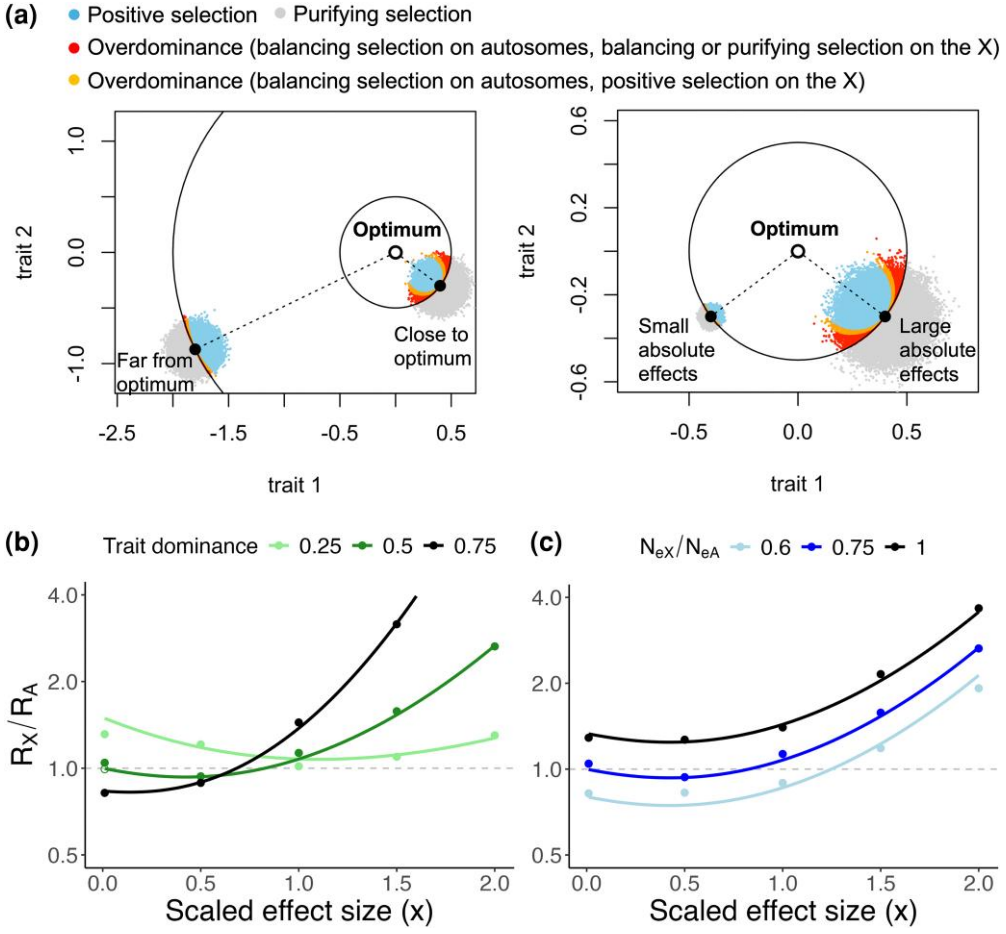


Fig. 1. Theoretical background. a) Two-dimensional representation of adaptation in Fisher's geometric model, showing an ancestral phenotype (black dots) and an optimum (white dot). Homozygous and heterozygous fitness effects are Gaussian functions of the distance to the optimum, and the points represent heterozygous fitness effects. The evolutionary dynamics of the mutations (positive selection, purifying selection, balancing selection) depend on the mode of inheritance (autosomal or X-linked), expression in each sex, and trait dominance, with conditions outlined in McDonough et al. (2024). We show the case where mutations are expressed in both sexes, hemizygous and homozygous phenotypic effects are equivalent, and phenotypic effects of mutations are semi-dominant. The *scaled* phenotypic effect of a mutation (x) is a positive function of the absolute magnitude of the mutation (r) and trait dimensionality ($\sqrt{n}$), and a negative function of the distance to optimum (z). The left panel shows that mutations can have large x because they are close to the optimum ($z = 0.5$ left vs. $z = 2$ right), or because they have large absolute magnitudes ($r \approx 0.15\sqrt{n}$ left vs. $r \approx 0.03\sqrt{n}$ right). This can generate overdominant balancing selection on autosomes (red and yellow points) but positive selection on the X (yellow points). b) Relative rates of adaptive substitution on the X chromosome (R_X) and autosomes (R_A), on a log2 scale, plotted as a function of scaled phenotypic effect size (x) and phenotypic dominance. The curve is based on expressions for fixation probability in McDonough et al. (2024) (ie eq. (S21) for the X chromosome and eq. (S20) for autosomes), multiplied by 3/4 to account for enhanced mutational input on autosomes. Points represent Wright–Fisher simulations of positively selected mutations, with fitness effects generated in Fisher's geometric model ($n = 50$, $z = 1$). Mutations were introduced sequentially with probability $\frac{1}{1+R}$ and $\frac{R}{1+R}$ (for autosomes and the X, respectively, where $R = \frac{N_{eX}}{N_{eA}} = 0.75$) to account for differences in mutational input, and were run until at least 1,000 fixations occurred on each chromosome type. We assumed $N_{eA} = 10^5$, $N_f = \frac{2N_{eA}}{9-8R}$, $N_m = N_f \frac{9-8R}{16R-9}$, initial frequencies of $1/4N_f$ and $1/4N_m$ for autosomes, and $1/3N_f$ and $1/3N_m$ for the X (following the simulation procedure in Lasne et al. 2017). Filled points denote simulations with fixed phenotypic dominance; the open point denotes a simulation where phenotypic dominance values were drawn from a uniform distribution between 0 and 1. c) Same as B, except that $\frac{N_{eX}}{N_{eA}}$ was varied, with phenotypic dominance fixed at 0.5.

0.75 in the house mouse (*Mus musculus castaneus*) (Kousathanas et al. 2014), and roughly 0.75 in humans (*Homo sapiens*) (Veeramah et al. 2014)—and in which strong faster-X adaptation has previously been reported.

Results

In *D. melanogaster*, one plausible explanation for faster-X adaptation is that genome-wide achiasmy in males elevates N_{eX}/N_{eA} to such a degree that there is no need to invoke recessive beneficial mutations

Downloaded from academic.oup.com/gbe/article/18/10/evag259/8907347 by library@ist.ac.at user on 23 October 2026

(Vicoso and Charlesworth 2009; Charlesworth et al. 2018). We therefore began by examining the relationship between N_{eX}/N_{eA} ratios and the extent of faster-X adaptation in this species. Specifically, Hill–Robertson interference reduces N_e in proportion to the extent of recombination, so that recombination rates can be used as proxies for local N_e (Charlesworth 2009). We estimated rates of adaptive substitution in different windows of recombination rate (each window containing roughly 150,000 coding sites; see Materials and Methods), after multiplying recombination rates by ½ on autosomes and 2/3 on the X to obtain "effective" recombination rates for each chromosome type and window. Rates of adaptive substitution for nonsynonymous sites were calculated as ω_a, using a modern version of the MK (see Materials and Methods), with *D. simulans* as the outgroup, polarizing substitutions using *D. simulans* and *D. yakuba,* and correcting for possible biases due to segregating deleterious and beneficial mutations by fitting a distribution of fitness effects (DFE) to unfolded site frequency spectra. As found previously (eg Campos et al. 2014; Castellano et al. 2016), effective recombination rates were higher on the X chromosome (mean cM/Mb = 1.97) than autosomes (mean cM/Mb = 1.09; see figure captions for results of all statistical tests). Moreover, rates of adaptation were positively correlated with recombination rate on both chromosome types (Fig. 2). However, a strong signal of faster-X adaptation was still observed in windows with the *same* effective recombination rate on the X and autosomes, implying that higher average effective recombination rates on the X are not a sufficient explanation for faster-X adaptation.

To test the hypothesis that scaled phenotypic effects influence the extent of faster-X adaptation, we used three proxies for scaled phenotypic effects. First, we used differences in the physico-chemical properties of amino acid pairs, measured by their "Grantham's distance" (Grantham 1974)—the rationale being that mutations with larger Grantham's distances should have larger absolute phenotypic effects (see right panel of Fig. 1a) and thus larger scaled phenotypic effects. Second, we used differences in amino acid conservation among nonsynonymous sites, measured by their "SIFT score" (Vaser et al. 2016), and differences in the age of genes that nonsynonymous sites fall in, with gene age inferred from phylogenetic patterns of gene orthology (Domazet-Lošo et al. 2017). The rationale here is that mutations in more conserved sites, or mutations in older genes, should be closer to their optimum, tending to increase their scaled phenotypic effects (see left panel of Fig. 1a).

To support the validity of our proxies, we took two approaches. We first correlated each metric with

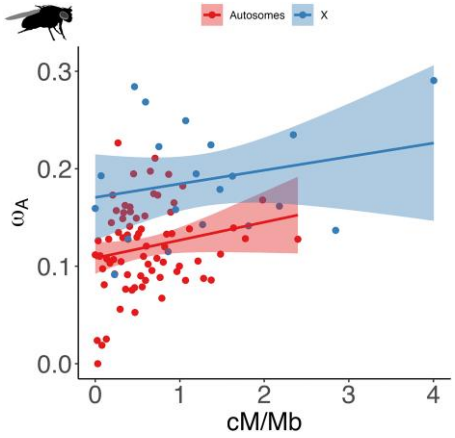


Fig. 2. Effective recombination rates and relative rates of X and autosome adaptation in *D. melanogaster*. Estimates of ω_a for each window of effective recombination rate (ie raw recombination rates in Comeron et al. (2012), multiplied by ½ on autosomes and 2/3 on the X chromosome; sites were binned into 20 windows of effective recombination rate on the X and 75 windows on autosomes; points represent the mean effective recombination rate of the window). Estimates of ω_a use the GammaExpo model to fit a DFE to segregating polymorphisms (see Materials and Methods). Negative estimates of ω_a were coded as zeroes. On average, recombination rate was higher on the X (Wilcoxon test, $W = 72{,}904$, $P < 0.001$). The linear regression coefficient for the effect of effective recombination rate on ω_a (lines) was $\beta = 0.016 \pm 0.008$ ($P = 0.041$). Residual ω_a (after correcting for recombination rate) was 0.039 on the X and −0.009 on autosomes (Wilcoxon test, $W = 386$, $P < 0.001$).

π_N/π_S, a measure of the efficiency of purifying selection (Castellano et al. 2018). In Fisher's geometric model, mutations with larger scaled phenotypic effects (Fisher 1930; Orr 1998) are more likely to evolve under purifying selection, so that we expect large-effect mutations (inferred based on our proxies) to be under stronger purifying selection than small-effect mutations. Accordingly, we found that π_N/π_S was strongly reduced among mutations with high amino acid dissimilarity (Fig. 3a), in highly conserved sites (Fig. 3b), and in older genes (Fig. 3c). In the case of Grantham's distances and gene age, this validation approach is robust, since the data used to generate both metrics and π_N/π_S are independent. In the case of SIFT scores (and related scores such as GERP or PhyloP), they are not strictly independent from π_N/π_S, given that an evolutionary genetic model of purifying selection was used to generate these scores in the first place (Huber et al. 2020) and the strength of purifying selection is phylogenetically correlated (Chen et al. 2017; Rousselle et al. 2020). This non-independence may therefore contribute to the correlation between SIFT categories and π_N/π_S.

Our second approach to validate the proxies was to examine the proportion of new mutations that are

Downloaded from academic.oup.com/gbe/article/18/10/evag259/8907347 by library@ist.ac.at user on 23 October 2026

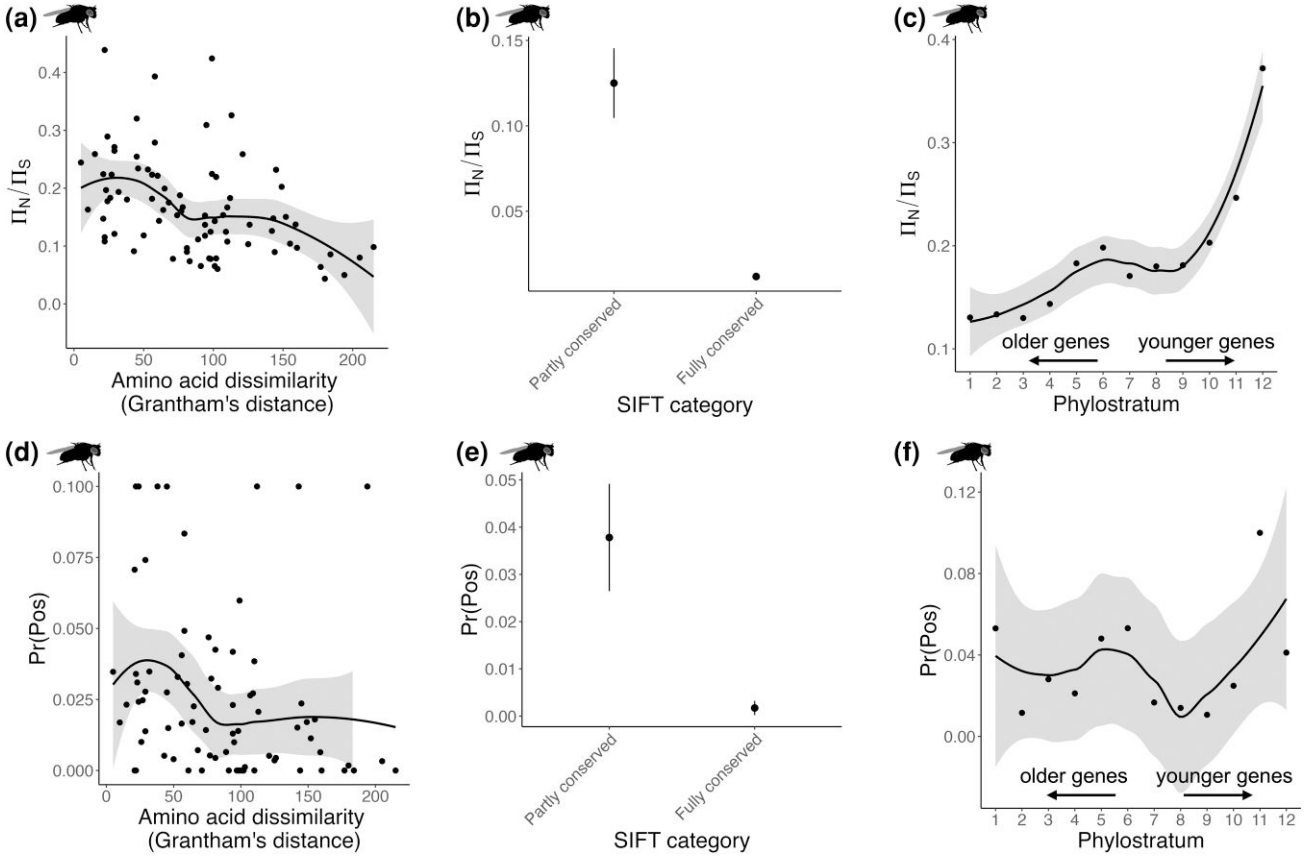


Fig. 3. Proxies for effect size and ratios of autosomal nonsynonymous to synonymous nucleotide diversity in *D. melanogaster*. a) Point estimates of autosomal π_N/π_S, for polymorphisms affecting 81 pairs of amino acids, ranked by their Grantham's distance, fitted with a loess regression curve. A significant negative rank correlation was observed (Spearman's $\rho = -0.461$, $P < 0.001$). This was also found on the X (Spearman's $\rho = -0.446$, $P < 0.001$; not shown). b) Same as (a), but autosomal π_N/π_S was compared between "Partly conserved" and "Fully conserved" SIFT score categories ($P < 0.001$, based on splitting the autosomal coding sequence into n bins with length equivalent to the X-linked coding sequence, and resampling autosomal estimates across these bins; points show the mean ± one bootstrap standard error). c) Same as (a), but autosomal π_N/π_S point estimates were compared between sites found in genes of varying phylostrata. Phylostratum 1 refers to "old" genes that are conserved across all cellular organisms, while phylostratum 12 represents "young" genes that are only found in Diptera. A significant positive correlation was observed between phylostratum and autosomal π_N/π_S (Spearman's $\rho = 0.874$, $P < 0.001$) corresponding to stronger purifying selection among older genes. This was also found for the X (Spearman's $\rho = 0.860$, $P < 0.001$; not shown). d) Same as (a), except shown for the proportion of sites under positive selection ("Pr(Pos)") on autosomes as a function of Grantham's distance (Spearman's $\rho = -0.359$, $P = 0.001$). This correlation was also found on the X (Spearman's $\rho = -0.468$, $P < 0.001$; not shown). e) Same as (b), except shown for Pr(Pos) as a function of SIFT score ($P < 0.001$). f) Same as (c), except shown for Pr(Pos) as a function of gene age on autosomes (Spearman's $\rho = 0.056$, $P = 0.869$) and the X (Spearman's $\rho = 0.504$, $P = 0.214$; not shown).

under positive selection (as estimated by fitting a DFE to unfolded site frequency spectra; see Materials and Methods) for mutations of different effect sizes. In Fisher's geometric model, mutations with large scaled phenotypic effects are predicted to be less often under positive selection (Fisher 1930; Orr 1998)—and indeed, we found that large-effect mutations were less likely to be under positive selection for each of the three proxies (Fig. 3d–f) (see also similar results in Bergman and Eyre-Walker 2019; Chen et al. 2022; Moutinho et al. 2022; Nocchi et al. 2024), although the relationships are somewhat noisier than for π_N/π_S. We refrain from quantitatively estimating scaled phenotypic effects based on the proportion of mutations under positive selection (an assumption-laden exercise; see Materials and Methods), but this is in principle possible, as we show in Fig. S16. In any case, the key point is that the *relative* values of our proxies tell us something about *relative* values of scaled phenotypic effects.

Having confirmed that our proxies for mutational effect size behave as expected, we correlated X-linked and autosomal rates of adaptation with each proxy (see Materials and Methods for details). We replicated the negative correlation between ω_a and effect size found

Downloaded from academic.oup.com/gbe/article/18/10/evag259/8907347 by library@ist.ac.at user on 23 October 2026

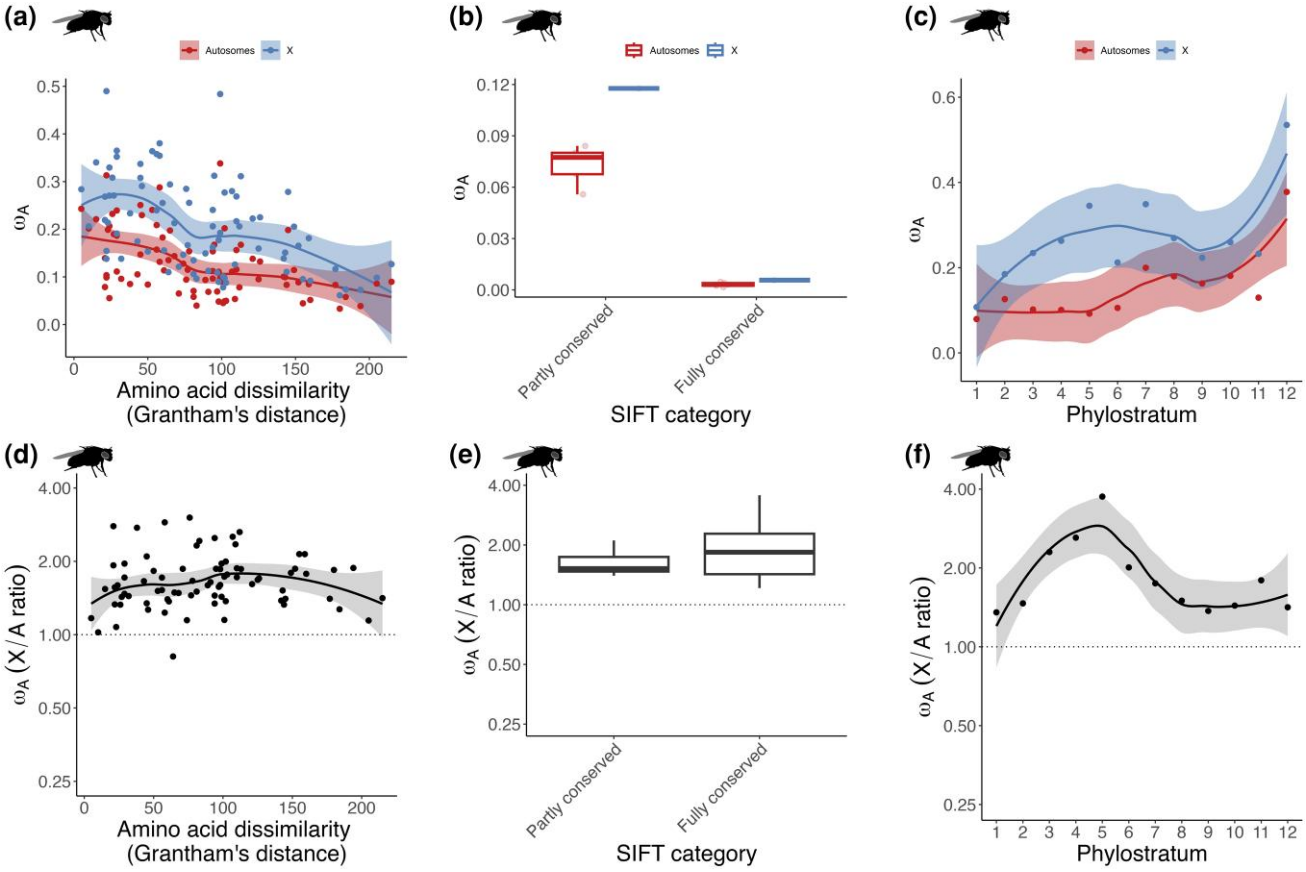


Fig. 4. Proxies for effect size and relative rates of X andautosome adaptation in *D. melanogaster*. a) Point estimates of rates of adaptation, ω_a, for nonsynonymous mutations affecting 81 pairs of amino acids, plotted against the Grantham's distance between each amino acid pair. b) Same as (a), but for nonsynonymous mutations categorized as having "Partly conserved" or "Fully conserved" SIFT scores (boxplots were obtained by splitting the autosomal coding sequence into *n* bins with length equivalent to the X-linked coding sequence, and resampling estimates of ω_a across these bins). c) Same as (a), but for nonsynonymous mutations that fall in genes with different Phylostrata (smaller values indicate that genes are older). d) Correlation between X/A ratios of ω_a and Grantham's distance (Spearman's $\rho = 0.129$, $P = 0.250$), with X/A ratios plotted on a log2 scale. Negative values of ω_a were treated as zeroes and infinite values were treated as 10^3. e) X/A ratios of ω_a vs. SIFT score category ($P = 0.436$, obtained by splitting the autosomal coding sequence into *n* bins with length equivalent to the X-linked coding sequence, resampling estimates of the X/A ratio of ω_a across these bins, and then calculating how many resampled estimates were larger in the "Fully conserved" than the "Partly conserved" SIFT category). f) Correlation between X/A ratios of ω_a and Phylostratum (Spearman's $\rho = -0.203$, $P = 0.528$).

previously in *D. melanogaster* (Fig. 4a–c) (Bergman and Eyre-Walker 2019; Moutinho et al. 2022), along with the strong signal of faster-X adaptation (Ávila et al. 2014; Campos et al. 2014; Charlesworth et al. 2018). However, we found no significant correlation between effect size and X/A ratios of ω_a, whether using Grantham's distances (Fig. 4d), SIFT scores (Fig. 4e), or gene age (Fig. 4f) as the metric of effect size. We repeated the analyses on 0- and 4-fold degenerate sites only (Fig. S1), using folded site frequency spectra rather than unfolded site frequency spectra when estimating the DFE (Fig. S2), using a more distant outgroup (*D. yakuba*, rather than *D. simulans*) (Figs. S3 and S4), and splitting our data by sex-biased gene expression (Figs. S5–S7). We found no evidence of a relationship between X/A ratios of ω_a and proxies for effect size, regardless of analysis strategy.

D. melanogaster is perhaps the ideal organism to test our hypothesis due to its highly polymorphic coding sequence and its relatively large X chromosome. Still, we were curious to see if our results generalize across species. We therefore repeated our analyses (using Grantham's distances and SIFT scores) in two species where faster-X adaptation has previously been reported (Kousathanas et al. 2014; Veeramah et al. 2014): the house mouse (*M. musculus castaneus*) and humans. Although noisier, data from both species mirror those in *D. melanogaster* (Fig. 5a–d). We found a negative correlation between effect size and π_N/π_S and ω_a (Fig. S8), both on the X and autosomes, and we recovered the

Downloaded from academic.oup.com/gbe/article/18/10/evag259/8907347 by library@ist.ac.at user on 23 October 2026

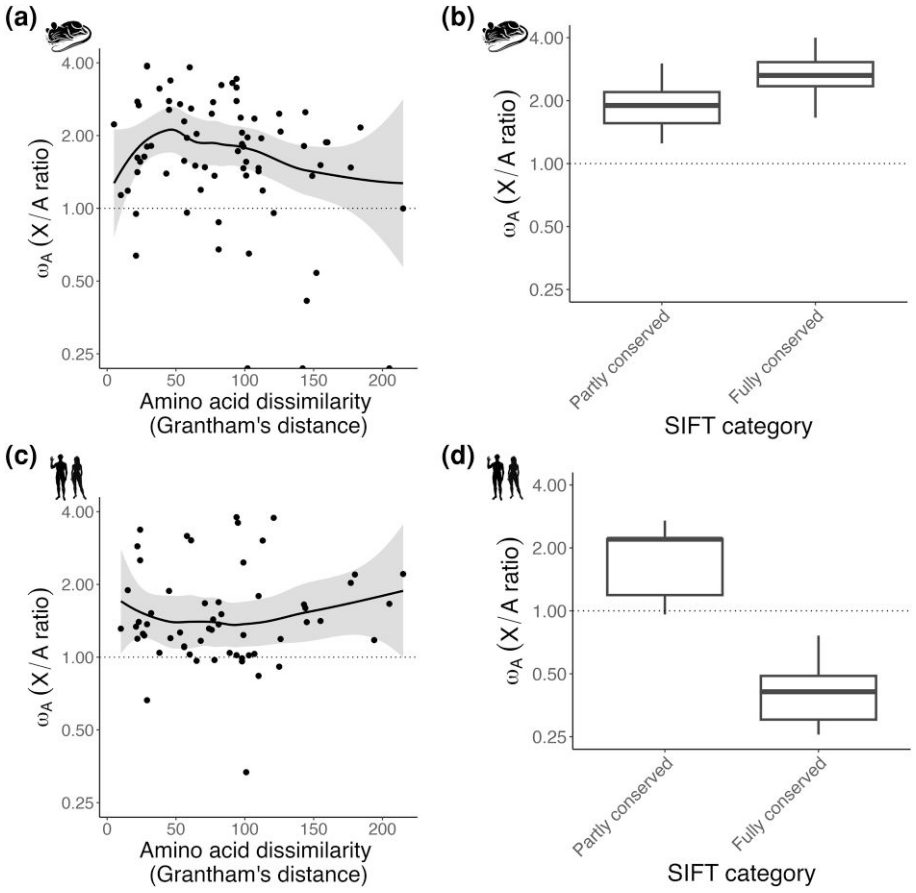


Fig. 5. Proxies for effect size and relative rates of X andautosome adaptation in *M. musculus* and *H. sapiens*. a) Point estimates of X/A ratios of rates of adaptation, ω_a, for nonsynonymous mutations affecting 81 pairs of amino acids, plotted against the Grantham's distance between each amino acid pair, in *M. musculus*. X/A ratios are plotted on a log2 scale. Negative values of ω_a were treated as zeroes and Infinite values were treated as 10^3 (Spearman's $\rho = -0.239$, $P = 0.032$). b) X/A ratios of ω_a vs. SIFT score category ($P = 0.136$, obtained by splitting the autosomal coding sequence into n bins with length equivalent to the X-linked coding sequence, resampling estimates of the X/A ratio of ω_a across these bins, as shown by the boxplots, and calculating how many resampled estimates were larger in the "Fully conserved" than the "Partly conserved" SIFT category). c) Same as (a), but for *H. sapiens* (Spearman's $\rho = 0.126$, $P = 0.260$) d) Same as (b), but for *H. sapiens* ($P = 0.879$, using the same statistical approach as in b.

strong faster-X signals reported previously. However, we found little in the way of significant correlations between effect size and X/A ratios of ω_a (Fig. 5a–d). One exception was a marginally significant ($P = 0.032$) *negative* correlation between Grantham's distance and X/A ratios of ω_a in *M. musculus*, but this was nonsignificant when using folded site frequency spectra to estimate the DFE (Fig. S9). In general, we observed no significant relationships between effect size and X/A ratios of ω_a, using different analysis strategies (Figs. S9–S15).

Discussion

Faster-X adaptation is a pervasive pattern in genome evolution (Meisel and Connallon 2013; McDonough et al. 2024). The most commonly invoked explanation —that new beneficial mutations are, on average, partially recessive (Charlesworth et al. 1987, 2018)—is at odds with theories of dominance for fitness, which predict that new beneficial mutations should usually be partially dominant and/or overdominant for fitness (Manna et al. 2011). Sex differences in recombination, or sex differences in variance in reproductive success (Vicoso and Charlesworth 2009) may contribute to the effect, but they are at best partial explanations, especially in species where N_{eX}/N_{eA} ratios are equal to or smaller than ¾ (Carneiro et al. 2012; Hvilsom et al. 2012; Garrigan et al. 2014; Kousathanas et al. 2014; Veeramah et al. 2014; Pinharanda et al. 2019). Models of adaptation from standing genetic variation are even less promising, since they predict faster-autosome adaptation even when new beneficial mutations

Downloaded from academic.oup.com/gbe/article/18/10/evag259/8907347 by library@ist.ac.at user on 23 October 2026

are partially recessive (Orr and Betancourt 2001). Here, we tested a new hypothesis: that faster-X adaptation arises due to large-effect mutations (McDonough et al. 2024). In McDonough et al.'s (2024) model, mutations with large scaled phenotypic effects can experience positive selection on the X even though equivalent mutations on autosomes experience balancing selection (and thus fail to fix) (Pamilo 1979). We tested the theory in three species (*D. melanogaster*, *M. musculus castaneus* and *H. sapiens*), using various proxies for mutational effect size (ie physico-chemical distances between amino acid-changing mutations, degrees of amino acid conservation, and gene ages). Although we were able to replicate the faster-X effect in each species (Ávila et al. 2014; Campos et al. 2014; Kousathanas et al. 2014; Veeramah et al. 2014), we found no significant correlations between our proxies for scaled phenotypic effects and the extent of faster-X adaptation.

Why did we fail to detect positive correlations between our effect size proxies and the extent of faster-X adaptation? One possible explanation is that beneficial mutations are typically recessive (a possibility we return to below) and have small "scaled phenotypic effects" (see Fig. 1b). It is difficult to assess whether scaled phenotypic effects are likely to be large or small in general, as this depends on assumptions about the distribution of absolute phenotypic effects of mutations, mutational correlations among them, the number of independent traits, and the distance to the phenotypic optimum (Orr 1998). One argument against the idea that they are small is that most new mutations are deleterious. For example, mutation accumulation studies find that ~90% of new mutations are deleterious (Bao et al. 2022), and fitting models of the DFE to nonsynonymous allele frequency spectra reveals a similarly high fraction of deleterious mutations (see Fig. 3d–f). This observation conflicts with infinitesimally small scaled phenotypic effects, because half of new mutations should be deleterious and half should be beneficial in Fisher's geometric model when this is the case (Orr 1998). The low proportion of new mutations that are beneficial instead suggests that scaled phenotypic effects will often be large (see Fig. S16).

Another possible contributor to our negative results is the difficulty of accurately estimating scaled phenotypic effects. We have relied on proxies, which are intended to capture variation in absolute phenotypic effects (ie Grantham's distances) or in the distance to the optimum (ie SIFT scores, gene age). These proxies are imperfect. For example, different components of scaled phenotypic effects might tradeoff with one another (eg mutations in older genes of *D. melanogaster* have smaller Grantham's distances and are more pleiotropic than younger genes, Moutinho et al. 2022; Martin and Tate 2025), which might dampen any genuine signal. Moreover, the power of conservation-based scores depends on the multiple sequence alignments used to generate these scores, and power will only be high when the total branch length of the tree is long (Huber et al. 2020). Our choice of conservation score, SIFT, is informed by the fact that it models the codon-based structure of protein-coding genes—in contrast to DNA-sequence-based metrics of conservation, such as GERP scores, which ignore this structure—but on the other hand, it ignores noncoding regions of the genome entirely (Huber et al. 2020). DNA-sequence-based conservation scores, like GERP, represent a promising avenue to further test McDonough et al.'s theory. Another problem is that our proxies do not necessarily capture the full range of scaled phenotypic effects. For example, mutations with the smallest Grantham's distances might still have large scaled phenotypic effects (see Fig. S16), which would then, under McDonough et al.'s theory, lead to faster-X adaptation across the range of Grantham's distances. But even if this is true, an observation that requires explanation is the absence of a correlation (negative or positive) between effect size and faster-X, which fits poorly with McDonough et al.'s theory (see dark green line with $v = 0.5$ in Fig. 1b).

Another way to approach our negative results is to consider direct data on dominance, which is an essential determinant of the relative behavior of autosomal and X-linked genes (Fig. 1b). Although there is a well-established observation that new deleterious mutations are partially recessive (Simmons and Crow 1977; Charlesworth 1979; Orr 1991; Agrawal and Whitlock 2011; Manna et al. 2011), data on phenotypic dominance, or on the dominance of beneficial mutations, are much sparser (Orr 2010; Billiard et al. 2021; Di and Lohmueller 2024). In the case of mutations conferring pesticide resistance in *Drosophila*, Bourguet and Raymond (1998) found that most mutations generate enough enzyme activity to be dominant for survival, while Ronfort and Glémin (2013) found a similar pattern when looking at quantitative trait loci affecting domestication in outcrossing plants. However, both estimates suffer from the well-known bias toward the fixation of dominant mutations in outcrossing diploids (ie Haldane's sieve, Haldane 1927; Orr and Betancourt 2001). In the same study by Ronfort and Glémin (2013), phenotypic dominance was also estimated among self-fertilizing plants, where Haldane's sieve should be minimal (Charlesworth 1992). There, they found a distribution shifted toward partially recessive effects. As these authors point out, however, it is not clear how domestication is related to total fitness, so to extrapolate from their estimates to dominance for fitness requires some caution.

Downloaded from academic.oup.com/gbe/article/18/10/evag259/8907347 by library@ist.ac.at user on 23 October 2026

Further direct estimates of the dominance of beneficial mutations come from evolution experiments in *S. cerevisiae*. In the case of haploid yeast lineages adapting to the antifungal fluconazole, roughly half of the ~30 adaptive mutations identified were recessive when they were expressed in diploids, while the other half were dominant (Anderson et al. 2004). For a dozen mutations conferring adaptation to nystatin, all were recessive (Gerstein et al. 2014). However, the candidate mutations identified in these experiments were often loss-of-function mutations affecting a single genetic pathway. Such loss-of-function mutations, though common in microbial evolution experiments (Behe and Dykhuizen 2010), are unlikely to represent the genetic basis of adaptation across a broad set of environments, and such mutations should contribute minimally to signals of molecular adaptation based on MK tests. Accordingly, further experiments conducted in different environments have found that candidate adaptive mutations often exhibit dominance or overdominance for fitness (Sellis et al. 2016; Marad et al. 2018; Aggeli et al. 2022). Overall, direct data on the dominance of new beneficial mutations remains exceptionally patchy, and there is a pressing need for larger-scale data in a range of contexts of selection to help parameterize models of adaptation (Orr 2010). "Deep mutational scanning" approaches (Padhy et al. 2023; Allen et al. 2026), in which a large number of mutations are generated in haploid vs. diploid state, and their fitness effects are inferred (eg from allele frequency trajectories among competing clones) offer promise in this regard.

Indirect inferences into the dominance of beneficial mutations have also been made by contrasting X and autosome adaptation among genes with male-biased vs. female-biased fitness effects. In Charlesworth et al.'s (2018) classical model of faster-X adaptation, mutations that are only expressed in females are expected to evolve equally fast on autosomes and the X, while mutations that are only expressed in males are expected to show a strong faster-X effect. Evidence that genes with male-biased expression experience stronger faster-X adaptation is mixed: it is observed in *D. melanogaster* (Campos et al. 2018) and *M. musculus* (Kousathanas et al. 2014), but not in *H. sapiens* (Veeramah et al. 2014) or *H. melpomene* (Pinharanda et al. 2019) (a ZW system, in which the prediction applies to female-biased genes). The weak relationship between faster-X adaptation and sex-biased gene expression is unsurprising, given that sex-biased expression is (at best) an imperfect proxy for sex-specific fitness effects. For example, sex-biased gene expression is positively related to metrics of sex-differential selection in some datasets (Connallon and Clark 2011), while other datasets find no (Ming et al. 2025), mixed (Grieshop et al. 2025), or negative (Ruzicka et al. 2019) associations. Still, establishing whether faster-X adaptation typically occurs for mutations with male-limited effects will be a valuable avenue for further work, given that McDonough et al.'s (2024) model only predicts faster-X under male-limited expression if new mutations show recessivity at the trait level.

Faster-X models typically consider scenarios where adaptation is limited by the supply of new mutations, but it is plausible that adaptation uses preexisting genetic variation (Barrett and Schluter 2008). But from the perspective of faster-X, adaptation from standing genetic variation is even less conducive to faster-X than mutation-limited models (Orr and Betancourt 2001; Connallon et al. 2012). For example, Orr and Betancourt (2001) considered a population with standing genetic variation maintained at a balance between recurrent mutation and purifying selection. The population then experiences a sudden shift in environmental conditions, such that deleterious alleles become beneficial while retaining the same dominance coefficient in the old and new environment. In this model, X-linked substitution rates are invariably lower than autosomal substitution rates. Not only do X-linked mutations suffer from reduced mutational input (as they do in mutation-limited models), but they are further hampered by their lower initial frequencies at the time of the environmental shift. Still, there is currently no thorough theoretical exploration of X and autosomal substitution rates in scenarios in which adaptation involves the simultaneous segregation of many mutations (eg polygenic models of stabilizing selection at a fixed optimum—Barton and Turelli 1989; stabilizing selection of a randomly fluctuating optimum—Bertram and Shafiei 2026; adaptation to a sudden shift in optimum—Hayward and Sella 2022), including cases where dominance changes between old and new environments (Muralidhar and Veller 2022). Such theory would be extremely valuable to identify conditions, if any, that facilitate faster-X adaptation when adaptation is not mutation-limited (see a recent simulation study by Muralidhar and Coop 2023 for a step in this direction), and it might help interpret the apparent enrichment of hard and soft sweeps on the X and autosomes, respectively (Harris and Garud 2023).

Another important theoretical assumption in models of faster-X is that the fitness effects of beneficial mutations in hemizygous males are equivalent to those in homozygous females. This assumption is well supported by data from the UK Biobank in humans (Sidorenko et al. 2019), in which the phenotypic effects of X-linked hemizygous mutations in males are typically equivalent to X-linked homozygous effects in females. However, there is wide variation in the mechanisms and the extent of dosage compensation across species

Downloaded from academic.oup.com/gbe/article/18/10/evag259/8907347 by library@ist.ac.at user on 23 October 2026

(Cecalev et al. 2024), which may influence the relative fitness effects of mutations between females and males on the X chromosome. For example, there is a suggestive pattern of weaker faster-Z than faster-X adaptation across species (McDonough et al. 2024), which might (among other explanations) be influenced by the extent of dosage compensation in ZW systems (often incomplete, eg in many birds and butterflies) vs. XY systems (complete in *Drosophila*, mostly complete in mammals). Empirical work investigating how variation in dosage compensation is related to the phenotypic and fitness effects of mutations (and thus, presumably, to patterns of X-linked variation and selection) is needed to properly test this hypothesis.

Finally, our inferences about rates of adaptation rely on the MK test, which is a robust (Booker 2020) but not infallible tool. On the one hand, some potential biases of the MK test (eg the assumption that the DFE is stable on the timescale of divergence) are alleviated by X-autosome contrasts, since such biases should apply equally to both chromosome types. On the other hand, X-autosome contrasts introduce new complications. For example, a standard assumption in current implementations of the MK test is that segregating functional polymorphisms are either neutral, unconditionally deleterious, or unconditionally beneficial (Eyre-Walker and Keightley 2009; Galtier 2016). Yet, segregating functional polymorphisms may also be overdominant (Sellis et al. 2011; McDonough and Connallon 2023; McDonough et al. 2024; Ruzicka et al. 2026). If overdominant polymorphisms are enriched on autosomes, as predicted by theory (Pamilo 1979), this "hidden" overdominance could exacerbate signals of faster-X adaptation. To our knowledge, X-autosome contrasts have only been performed among candidates for long-term balancing selection in humans, and such candidate loci are equally abundant on both chromosome types (see Supplementary Materials in Leffler et al. 2013). Whether the lack of enrichment applies to targets of short-term balancing selection (Soni et al. 2022), and whether this appreciably distorts MK tests, remains to be investigated.

Materials and Methods

Divergence Data

Our three focal species were *D. melanogaster*, *M. musculus*, and *H. sapiens*. The relevant reference assemblies were number 5 for *D. melanogaster* (GCF_000001215.2), GRCm38 for *M. musculus* (GCF_000001635.20), and GRCh38 for *H. sapiens* (GRCh38.p14). For each focal species, we obtained DNA and protein sequences for all transcripts using gffread (Pertea and Pertea 2020), a tool that takes the gff and fasta files for each species' reference as input and considers the strand and reading frame of each transcript. For each gene, we removed all but the longest transcript, using custom bash scripts. To identify substitutions, we used two outgroups for each lineage: *D. simulans* and *D. yakuba*, which have diverged from *D. melanogaster* 1 to 4 million years ago (MYA) and 2 to 9 MYA, respectively (Obbard et al. 2012; Suvorov et al. 2022); *M. spretus* and *M. pahari*, which have diverged from *M. musculus* 1 to 2 MYA and 5 to 7 MYA, respectively (Suzuki et al. 2004; Thybert et al. 2018); and *Pan troglodytes* and *Gorilla gorilla*, which have diverged from humans 7 to 8 MYA and 11 to 17 MYA, respectively (Langergraber et al. 2012). In each lineage, we identified 1:1:1 orthologs using orthofinder (Emms and Kelly 2019), resulting in 11,716 orthogroups for the *Drosophila* lineage, 14,862 for the mouse lineage and 14,949 for the primate lineage. We then aligned each orthogroup in turn, using the codon-aware multiple sequence aligner MACSE (Ranwez et al. 2011). We recovered the position of every site in terms of the coordinates of the focal species' reference genome, using custom bash scripts. We only considered substitutions (eg between *D. melanogaster* and *D. simulans*) that were non-polymorphic in the focal species (eg in *D. melanogaster*).

Polymorphism Data

For *D. melanogaster*, we used single nucleotide polymorphism (SNP) data from a Zambian population sample (DPGP3), downloaded from www.johnpool.net/genomes.html. The sample consists of 197 haploid genome sequences from *D. melanogaster*'s ancestral distribution range, and is minimally affected by the bottlenecks accompanying *D. melanogaster*'s expansion out of Africa (Arguello et al. 2019). Details of the SNP calling pipeline can be found in Lack et al. (2016). For each major chromosome arm, the multiple-alignment fasta files were converted to vcf using snp-sites (Page et al. 2016), and coding regions were extracted using bedtools (Quinlan and Hall 2010). We obtained allele counts for polymorphic sites using vcftools (Danecek et al. 2011), retaining only biallelic sites, sites with call rate >80% across individuals, and sites where at least one of the polymorphic alleles matches the transcribed allele in the reference assembly, using custom R scripts (RStudio Team 2020). Because alleles in the polymorphism dataset are reported with respect to the forward strand (even if transcription takes place on the reverse strand), we converted alleles to their complement whenever the site was transcribed from the reverse strand (eg if a C/T polymorphism was transcribed from the reverse strand, we converted it to a G/A polymorphism).

Downloaded from academic.oup.com/gbe/article/18/10/evag259/8907347 by library@ist.ac.at user on 23 October 2026

For *M. musculus*, we used polymorphism data from a sample of 10 diploid individuals of the sub-species *M. musculus castaneus*, whose ancestral distribution range is in India and whose N_e is inferred to be larger than *M. musculus domesticus* (Halligan et al. 2010). Reads had previously been mapped to the GRCm38 reference assembly (see Harr et al. 2016 for details) and were downloaded from wwwuser.gwdguser.de/~evolbio/evolgen/wildmouse/vcf/. We applied the same filters as in *D. melanogaster*, and we further removed pseudo-autosomal regions (positions 90,745,845–91,644,698 and 169,969,759–170,931,299; per https://ftp.ncbi.nlm.nih.gov/genomes/all/GCF/000/001/635/GCF_000001635.20_GRCm38/GCF_000001635.20_GRCm38_assembly_structure/genomic_regions_definitions.txt). For *H. sapiens*, we used polymorphisms from the 1000 genomes project (The 1000 Genomes Project Consortium 2015), aligned to the GRCh38 assembly, and downloaded from www.cog-genomics.org/plink/2.0/resources. We initially converted pgen files to vcf files using plink2 (Chang et al. 2015), and then proceeded as elsewhere, removing pseudo-autosomal regions as well (positions 10,001–2,781,479 and 155,701,383–156,030,895; per GCA_000001405.29_GRCh38.p14_assembly_structure/genomic_regions_definitions.txt).

We used parsimony to infer ancestral allele states at the node of the tree leading to each focal species. Specifically, we inferred an allele to be ancestral if both outgroup species (eg *D. simulans* and *D. yakuba*) carried the allele; the alternative allele was then assigned as the derived allele. In cases where the focal species carried an allele that was not present in the two outgroup species, we removed the polymorphism from further analysis. In cases where the more distant outgroup (eg *D. yakuba*) was used to estimate divergence, we inferred ancestral allele state based on this outgroup only.

Scaled Phenotypic Effects and Their Proxies

Before describing how we estimated the effect size of mutations, it is worth clarifying what kind of effect size we are aiming to measure, since there are many possible kinds in population genetics. For our purposes, the relevant effect size is a mutation's "scaled phenotypic effect" (x), which is formally defined as $x = \frac{r\sqrt{n}}{2z}$, where r is an absolute phenotypic effect (summed across a set of independent traits), n is the number of independent traits, and z is the distance from the phenotypic optimum (Orr 1998). Thus, mutations can have large "x" if they have large absolute phenotypic effects (ie large values of r), or if they are close to the optimum (ie small values of z), as illustrated in the left vs. right panels of Fig. 1a. Put simply, our first metric of effect size (Grantham's distances; see below) is intended to capture variation in absolute effect size (r), while our two other metrics (SIFT score and gene age; see below) are intended to capture variation in distance to the phenotypic optimum (z).

Values of x are very difficult to estimate empirically. Estimating x requires making assumptions about the distribution of absolute phenotypic effects, the number of independent traits, and mutational correlations among them. Moreover, if we model adaptation as an "adaptive walk," populations closer to the optimum should tend to fix mutations with smaller x than populations far from the optimum (Orr 1998; Moutinho et al. 2022), so that the value of x will also depend on assumptions about which step in the adaptive walk the population is in. Despite these limitations, proxies can still provide information about the *relative* values of x among different classes of mutation. Moreover, we can validate the proxies by asking whether large-effect mutations, thus inferred, show properties that are consistent with those predicted for large-x mutations in Fisher's geometric model. For example, a long-standing result (Fisher 1930) is that the proportion of mutations under purifying selection should increase as x increases. We tested this by asking whether large-effect mutations, inferred from our proxies, were more likely to be under purifying selection than small-effect mutations, using π_N/π_S, a common measure of the efficiency of purifying selection (Castellano et al. 2018). Another prediction is that the proportion of mutations under positive selection should decrease as x increases (Fisher 1930). The proportion of mutations under positive selection was estimated from fitting models of the distributions of fitness effects (DFE) to nonsynonymous and synonymous polymorphism data, using the software grapes (Galtier 2016) (see details below). Finally, by way of illustration, we present analytical predictions that relate the average value of x to the estimated proportion of mutations under positive selection (see Fig. S16).

Proxies for Mutational Effect Size

We used three metrics as proxies for scaled phenotypic effects. First, we partitioned nonsynonymous mutations by dissimilarity using Grantham's distances, downloaded from gist.github.com/danielecook/501f03650bca6a3db31ff3af2d413d2a#file-grantham-tsv. The Grantham's distance between a pair of amino acids is a composite measure of the dissimilarity in polarity, volume, and composition between them (Grantham 1974). In other words, it quantifies whether a mutation converts one amino acid (eg Isoleucine) to a very similar amino acid (eg Leucine) or to a very dissimilar amino acid (eg Serine). Thus, it should capture variation in

Downloaded from academic.oup.com/gbe/article/18/10/evag259/8907347 by library@ist.ac.at user on 23 October 2026

the absolute phenotypic effects of mutations. In practice, we predicted the effects of all possible coding mutations at every site in each focal species using degenotate (Mirchandani et al. 2024). Mutations (polymorphisms and substitutions) were then assigned a Grantham's distance using custom R scripts.

Second, we partitioned nonsynonymous mutations by their "Sorting Intolerant from Tolerant for Genomes" (SIFT) score (Ng and Henikoff 2001). SIFT is an algorithm to predict the functional consequences of mutations based on a protein sequence alignment with related species. Our rationale is that a highly conserved amino acid is likely to be close to its optimum, such that a mutation affecting a highly conserved amino acid should have a larger scaled phenotypic effect than a mutation affecting a weakly conserved amino acid (given that scaled phenotypic effects are inversely proportional to the distance to the optimum in Fisher's geometric model). Amino acids might also be highly conserved because there is systematic variation in the functional importance of different amino acids, in which case SIFT scores partly reflect variation in the absolute effects of mutations. Either way, SIFT scores have previously been used to partition putatively beneficial mutations into those of small and large effect (Chen et al. 2022). In practice, we used SIFT4G (Vaser et al. 2016) to calculate SIFT scores for each possible mutation at every coding site, using publicly available SIFT files (BDGP5.74, GRCm38.74, GRCh38.74, respectively, downloaded from https://sift.bii.a-star.edu.sg/sift4g/public/) and reference genome files (converted to vcf) as input. SIFT scores vary between 0 and 1 and are highly skewed toward 0. We assigned a SIFT score of 1 to reference alleles, and categorized large-effect ("partly conserved") mutations as those where the difference in SIFT scores between two alleles was >0.9999, and small-effect mutations ("fully conserved") as those where the difference in SIFT scores was 0.0499 to 0.9999.

Finally, we used a phylostratigraphic approach to classify nonsynonymous mutations. Mutations were binned by gene age into "old" genes that share homologs in distantly related species and "young" genes that only share homologs in closely related species. The rationale is that older genes should be closer to their optimum, such that mutations in older genes should have larger scaled phenotypic effects. To classify genes by age in *D. melanogaster*, we used the 12 phylostrata defined by Domazet-Lošo et al. (2017).

Rates of Adaptation

We used MK tests to estimate rates of adaptation (McDonald and Kreitman 1991). MK tests compare polymorphism (P_s) and divergence (D_s) at putatively neutral sites and polymorphism (P_N) and divergence (D_N) at putatively functional sites. If all new mutations at putatively functional sites are either neutral or strongly deleterious, then $\frac{D_N}{D_S} = \frac{P_N}{P_S}$. If some putatively functional mutations are adaptive, the number of excess substitutions due to positive selection can be estimated as $a = D_N - \frac{D_S P_N}{P_S}$ (Smith and Eyre-Walker 2002). In the absence of segregating non-neutral mutations, the proportion of putatively functional substitutions that are adaptive can then be estimated as $\alpha = \frac{a}{D_N} = 1 - \frac{D_S P_N}{D_N P_S}$, and the rate of adaptation (scaled by the rate of neutral substitution) is $\omega_a = \frac{a}{D_S}$ (Galtier 2016). We used ω_a as our focal metric of adaptation because it is a rate, rather than a proportion, and thus more directly relevant to the theory (similar results were found using α instead; not shown).

In practice, mildly deleterious mutations often segregate at putatively functional sites, which will downwardly bias estimates of α and ω_a (Keightley and Eyre-Walker 2007; Eyre-Walker and Keightley 2009). To correct for this, we fitted models of the DFE among putatively functional polymorphisms, using grapes (Galtier 2016). Specifically, we fitted the "GammaExpo" model, where segregating deleterious mutations are assumed to follow a gamma distribution (whose shape and scale parameters are estimated by grapes) and segregating beneficial mutations follow an exponential distribution. This model accurately estimates rates of adaptation (Booker 2020) and provides the best fit to unfolded allele frequency spectra in most species (Rousselle et al. 2020). To guard against misestimation of ancestral allele states, we repeated analyses on the folded allele frequency spectrum, fitting the "GammaZero" model, which considers that segregating beneficial mutations are absent and segregating deleterious mutations follow a gamma distribution. This model also provides an excellent fit in most species (Rousselle et al. 2020). Because DFE estimation in grapes does not handle large samples of sequences well, we down-sampled the allele frequency spectrum to a maximum of 20 sequences. We did this by splitting the full site frequency spectrum into 20 bins and multiplying counts in each bin by a factor $20/n$, where n is the number of sequences in the sample (eg 20/197 for *D. melanogaster* polymorphism data). Twenty sequences is sufficient for accurate inferences of the DFE and ω_a (Charlesworth and Eyre-Walker 2008), provided that the number of segregating sites per unit of analysis is large (on the order of 10^3 to 10^4 SNPs, per Andersson et al. 2023).

Grapes require a mutational target size as input. To estimate mutational target size, we considered the

Downloaded from academic.oup.com/gbe/article/18/10/evag259/8907347 by library@ist.ac.at user on 23 October 2026

base composition of coding sequences and transition-transversion (ts:tv) bias. Specifically, given that each base occurs at a fraction f in a focal species' coding sequence, we assumed the probability of a transversion to be $p_{tv} = \frac{(f_{tv}+f_{tv})}{2(1+t)}$ and the probability of a transition to be $p_{ts} = \frac{t(f_{ts}+f_{ts})}{1+t}$, where f_{tv} and f_{ts} are pairs of bases undergoing transversions and transitions, respectively, and t is the ts:tv ratio of mutation *counts*. Based on mutation accumulation data, we used $t = 1$ for *D. melanogaster* (Keightley et al. 2009) and $t = 2$ for *Mus* and humans (Kong et al. 2012; Lynch et al. 2023), corresponding to 2-fold and 4-fold higher transition *rates*, respectively. We estimated mutational target size for a given site class by summing all possible mutations of that class across a species' coding sequence, weighted by its mutation probability (given overall genomic base composition and relevant ts:tv ratios).

In many cases, mutations in a particular amino acid pair (eg Alanine to Valine) originate from a few (often just one) kind of mutation (eg C↔T), which can cause problems (when comparing across mutational classes) if there is codon usage bias (Singh et al. 2008; Vicoso et al. 2008) or GC-biased gene conversion (which typically favor G or C alleles Jackson et al. 2017; Rousselle et al. 2019). To account for this, we followed the approach of Bergman and Eyre-Walker (2019). Specifically, for a given amino acid pair, we used synonymous sites that are separated by the same mutation type as the neutral baseline, such that all relevant inputs for grapes consisted of that mutation type only (eg C↔T mutations only, for the Alanine to Valine amino acid pair). When an amino acid pair was separated by more than one mutation type (eg some mixture of C↔T and C↔G), we weighted synonymous sites by the relative frequency of each mutation type (eg if a given amino acid pair was predicted to originate via 50% C↔T and 50% C↔G mutations, the synonymous site frequency spectrum was weighted 50% to C↔T mutations and 50% to C↔G mutations).

Recombination Rates

In *D. melanogaster*, recombination rate estimates were obtained from Comeron et al. (2012), downloaded from https://comeron.lab.uiowa.edu/recombination-rates. The estimates are provided in 100 Kb windows, which can result in noisy estimates of ω_a if there are few coding sites in each window (Andersson et al. 2023). To minimize this effect, we assigned each site a recombination rate (eg a coding site falling into a 100 kb window with a recombination rate of 1 cM/Mb was assigned a recombination of 1 cM/Mb), ranked them by recombination rate, and binned them into 20 non-overlapping windows for the X, and 75 non-overlapping windows for the autosomes. Thus, each window-based estimate of ω_a used ~150 to 200 kb coding sites. Since recombination rates were estimated in females and there is no recombination in *Drosophila* males, we multiplied recombination rate estimates by 2/3 for the X and by ½ for autosomes. These corrections adjust for the fact that two-thirds of X-linked genes and one-half of autosomal genes are carried by females.

Sex-Biased Gene Expression

The sex-specific fitness effects of mutations should correlate with X-autosome ratios of adaptive substitution rates (Charlesworth et al. 2018), and sex-biased expression is often used as a proxy for the sex-specific fitness effects (whether this assumption is justified is something we return to in the Discussion). We therefore examined rates of adaptation among genes with different levels of sex-biased expression. We used expression data that has been pre-processed by Fraïsse et al. (2019). Briefly, the expression data consist of numbers of reads per kilobase per million reads (RPKM), obtained from Flybase ("gene_rpkm_report_fb_2017_04.tsv.gz"). These counts have been quantile-normalized between males and females, and between tissues for a given developmental stage. We then estimated the sex-bias ratio as Fraïsse et al. (2019) did, by estimating the mean of reproductive tissue samples in females (ovary samples among 4-day-old mated and virgin females) and males (accessory gland and testis samples among 4-day-old males), and taking the log2 ratio of the male-to-female values. Male-biased, female-biased, and unbiased genes were classified as genes with a log2 ratio greater than 1, smaller than −1, and between −1 and 1, respectively.

Supplementary Material

Supplementary material is available at *Genome Biology and Evolution* online.

Acknowledgments

We thank Tim Connallon for comments on a draft of this manuscript and for assistance with the theory presented in the Supplementary Materials.

Funding

F.R. was funded by a H2020 Marie Skłodowska Curie Actions fellowship (#101034413).

Downloaded from academic.oup.com/gbe/article/18/10/evag259/8907347 by library@ist.ac.at user on 23 October 2026

Data Availability

All data and code necessary for confirming the conclusions of the article can be found at https://github.com/filipluca/FasterX_and_mutation_size.

Literature Cited

Aggeli D, et al. Overdominant and partially dominant mutations drive clonal adaptation in diploid *Saccharomyces cerevisiae*. Genetics. 2022:221:iyac061. https://doi.org/10.1093/genetics/iyac061.

Agrawal AF, Whitlock MC. Inferences about the distribution of dominance drawn from yeast gene knockout data. Genetics. 2011:187:553–566. https://doi.org/10.1534/genetics.110.124560.

Allen MG, Martínez AA, Lang GI. Prevalence, distribution, and mechanisms of genetic dominance in the yeast mating pathway. Genetics. 2026:233:iyag105. https://doi.org/10.1093/genetics/iyag105.

Anderson JB, Sirjusingh C, Ricker N. Haploidy, diploidy and evolution of antifungal drug resistance in *Saccharomyces cerevisiae*. Genetics. 2004:168:1915–1923. https://doi.org/10.1534/genetics.104.033266.

Andersson BA, et al. Inference of the distribution of fitness effects of mutations is affected by single nucleotide polymorphism filtering methods, sample size and population structure. Mol Ecol Resour. 2023:23:1589–1603. https://doi.org/10.1111/1755-0998.13825.

Arguello JR, Laurent S, Clark AG. Demographic history of the human commensal *Drosophila melanogaster*. Genome Biol Evol. 2019:11:844–854. https://doi.org/10.1093/gbe/evz022.

Avery PJ. The population genetics of haplo-diploids and X-linked genes. Genet Res. 1984:44:321–341. https://doi.org/10.1017/S0016672300026550.

Ávila V, et al. Faster-X effects in two *Drosophila* lineages. Genome Biol Evol. 2014:6:2968–2982. https://doi.org/10.1093/gbe/evu229.

Baines JF, Sawyer SA, Hartl DL, Parsch J. Effects of X-linkage and sex-biased gene expression on the rate of adaptive protein evolution in *Drosophila*. Mol Biol Evol. 2008:25:1639–1650. https://doi.org/10.1093/molbev/msn111.

Baird RB, et al. Faster adaptation but slower divergence of X chromosomes under paternal genome elimination. Nat Commun. 2025:16:5288. https://doi.org/10.1038/s41467-025-60114-8.

Bao K, Melde RH, Sharp NP. Are mutations usually deleterious? A perspective on the fitness effects of mutation accumulation. Evol Ecol. 2022:36:753–766. https://doi.org/10.1007/s10682-022-10187-4.

Barrett RDH, Schluter D. Adaptation from standing genetic variation. Trends Ecol Evol. 2008:23:38–44. https://doi.org/10.1016/j.tree.2007.09.008.

Barton NH, Turelli M. Evolutionary quantitative genetics: how little do we know? Annu Rev Genet. 1989:23:337–370. https://doi.org/10.1146/annurev.ge.23.120189.002005.

Bechsgaard J, et al. Evidence for faster X chromosome evolution in spiders. Mol Biol Evol. 2019:36:1281–1293. https://doi.org/10.1093/molbev/msz074.

Behe MJ, Dykhuizen DE. Experimental evolution, loss-of-function mutations, and "the first rule of adaptive evolution". Q Rev Biol. 2010:85:419–445. https://doi.org/10.1086/656902.

Bergman J, Eyre-Walker A. Does adaptive protein evolution proceed by large or small steps at the amino acid level? Mol Biol Evol. 2019:36:990–998. https://doi.org/10.1093/molbev/msz033.

Bertram J, Shafiei Z. 2026.Strong amplification of quantitative genetic variation under a balance between mutation and fluctuating stabilizing selection. *Genetics*. 2026:233:iyag063. https://doi.org/10.1093/genetics/iyag063.

Billiard S, Castric V, Llaurens V. The integrative biology of genetic dominance. Biol Rev Camb Philos Soc. 2021:96:2925–2942. https://doi.org/10.1111/brv.12786.

Booker TR. Inferring parameters of the distribution of fitness effects of new mutations when beneficial mutations are strongly advantageous and rare. G3 (Bethesda). 2020:10:2317–2326. https://doi.org/10.1534/g3.120.401052.

Bourguet D, Raymond M. The molecular basis of dominance relationships: the case of some recent adaptive genes. J Evol Biol. 1998:11:103–122. https://doi.org/10.1046/j.1420-9101.1998.11010103.x.

Brengdahl M, Kimber CM, Maguire-Baxter J, Friberg U. Sex differences in life span: females homozygous for the X chromosome do not suffer the shorter life span predicted by the unguarded X hypothesis. Evolution. 2018:72:568–577. https://doi.org/10.1111/evo.13434.

Campos JL, et al. Codon usage bias and effective population sizes on the X chromosome versus the autosomes in *Drosophila melanogaster*. Mol Biol Evol. 2013:30:811–823. https://doi.org/10.1093/molbev/mss222.

Campos JL, Halligan DL, Haddrill PR, Charlesworth B. The relation between recombination rate and patterns of molecular evolution and variation in *Drosophila melanogaster*. Mol Biol Evol. 2014:31:1010–1028. https://doi.org/10.1093/molbev/msu056.

Campos JL, Johnston KJA, Charlesworth B. The effects of sex-biased gene expression and X-linkage on rates of sequence evolution in *Drosophila*. Mol Biol Evol. 2018:35:655–665. https://doi.org/10.1093/molbev/msx317.

Carneiro M, et al. Evidence for widespread positive and purifying selection across the European rabbit (*Oryctolagus cuniculus*) genome. Mol Biol Evol. 2012:29:1837–1849. https://doi.org/10.1093/molbev/mss025.

Castellano D, et al. Adaptive evolution is substantially impeded by Hill–Robertson interference in *Drosophila*. Mol Biol Evol. 2016:33:442–455. https://doi.org/10.1093/molbev/msv236.

Castellano D, James J, Eyre-Walker A. Nearly neutral evolution across the *Drosophila melanogaster* genome. Mol Biol Evol. 2018:35:2685–2694. https://doi.org/10.1093/molbev/msy164.

Cecalev D, Viçoso B, Galupa R. Compensation of gene dosage on the mammalian X. Development. 2024:151:dev202891. https://doi.org/10.1242/dev.202891.

Chang CC, et al. Second-generation PLINK: rising to the challenge of larger and richer datasets. GigaScience. 2015:4:7. https://doi.org/10.1186/s13742-015-0047-8.

Charlesworth B. Evidence against Fisher's theory of dominance. Nature. 1979:278:848–849. https://doi.org/10.1038/278848a0.

Charlesworth B. Evolutionary rates in partially self-fertilizing species. Am Nat. 1992:140:126–148. https://doi.org/10.1086/285406.

Charlesworth B. The effect of life-history and mode of inheritance on neutral genetic variability. Genet Res. 2001:77:153–166. https://doi.org/10.1017/S0016672301004979.

Charlesworth B. Fundamental concepts in genetics: effective population size and patterns of molecular evolution and variation. Nat Rev Genet. 2009:10:195–205. https://doi.org/10.1038/nrg2526.

Downloaded from academic.oup.com/gbe/article/18/10/evag259/8907347 by library@ist.ac.at user on 23 October 2026

Charlesworth B, Campos JL, Jackson BC. Faster-X evolution: theory and evidence from *Drosophila*. Mol Ecol. 2018:27:3753–3771. https://doi.org/10.1111/mec.14534.
Charlesworth B, Coyne J, Barton N. The relative rates of evolution of sex chromosomes and autosomes. Am Nat. 1987:130:113–146. https://doi.org/10.1086/284701.
Charlesworth J, Eyre-Walker A. The McDonald–Kreitman test and slightly deleterious mutations. Mol Biol Evol. 2008:25: 1007–1015. https://doi.org/10.1093/molbev/msn005.
Chase MA, Vilcot M, Mugal CF. Evidence that genetic drift not adaptation drives fast-Z and large-Z effects in Ficedula flycatchers. Mol Ecol. 2025:34:e17262. https://doi.org/10.1111/mec.17262.
Chen J, Bataillon T, Glémin S, Lascoux M. Hunting for beneficial mutations: conditioning on SIFT scores when estimating the distribution of fitness effect of new mutations. Genome Biol Evol. 2022:14:evab151. https://doi.org/10.1093/gbe/evab151.
Chen J, Glémin S, Lascoux M. Genetic diversity and the efficacy of purifying selection across plant and animal species. Mol Biol Evol. 2017:34:1417–1428. https://doi.org/10.1093/molbev/msx088.
Chevy ET, Huerta-Sánchez E, Ramachandran S. Integrating sex-bias into studies of archaic introgression on chromosome X. PLoS Genet. 2023:19:e1010399. https://doi.org/10.1371/journal.pgen.1010399.
Comeron JM, Ratnappan R, Bailin S. The many landscapes of recombination in *Drosophila melanogaster*. PLoS Genet. 2012:8: e1002905. https://doi.org/10.1371/journal.pgen.1002905.
Connallon T, Beasley IJ, McDonough Y, Ruzicka F. How much does the unguarded X contribute to sex differences in lifespan? Evol Lett. 2022:6:319–329. https://doi.org/10.1002/evl3.292.
Connallon T, Clark AG. Association between sex-biased gene expression and mutations with sex-specific phenotypic consequences in *Drosophila*. Genome Biol Evol. 2011:3:151–155. https://doi.org/10.1093/gbe/evr004.
Connallon T, Singh ND, Clark AG. Impact of genetic architecture on the relative rates of X versus autosomal adaptive substitution. Mol Biol Evol. 2012:29:1933–1942. https://doi.org/10.1093/molbev/mss057.
Danecek P, et al. The variant call format and VCFtools. Bioinformatics. 2011:27:2156–2158. https://doi.org/10.1093/bioinformatics/btr330.
Darolti I, et al. Sex chromosome heteromorphism and the Fast-X effect in poeciliids. Mol Ecol. 2023:32:4599–4609. https://doi.org/10.1111/mec.17048.
Di C, Lohmueller KE. Revisiting dominance in population genetics. Genome Biol Evol. 2024:16:evae147. https://doi.org/10.1093/gbe/evae147.
Domazet-Lošo T, et al. No evidence for phylostratigraphic bias impacting inferences on patterns of gene emergence and evolution. Mol Biol Evol. 2017:34:843–856. https://doi.org/10.1093/molbev/msw284.
Dutheil JY, et al. Strong selective sweeps on the X chromosome in the human-chimpanzee ancestor explain its low divergence. PLoS Genet. 2015:11:e1005451. https://doi.org/10.1371/journal.pgen.1005451.
Ellegren H. The different levels of genetic diversity in sex chromosomes and autosomes. Trends Genet. 2009:25:278–284. https://doi.org/10.1016/j.tig.2009.04.005.
Ellegren H, et al. The genomic landscape of species divergence in *Ficedula* flycatchers. Nature. 2012:491:756–760. https://doi.org/10.1038/nature11584.
Emms DM, Kelly S. OrthoFinder: phylogenetic orthology inference for comparative genomics. Genome Biol. 2019:20:238. https://doi.org/10.1186/s13059-019-1832-y.
Eyre-Walker A, Keightley PD. Estimating the rate of adaptive molecular evolution in the presence of slightly deleterious mutations and population size change. Mol Biol Evol. 2009:26: 2097–2108. https://doi.org/10.1093/molbev/msp119.
Fisher RA. The genetical theory of natural selection. Clarendon Press; 1930. https://doi.org/10.1038/158453a0.
Fraïsse C, Puixeu Sala G, Vicoso B. Pleiotropy modulates the efficacy of selection in *Drosophila melanogaster*. Mol Biol Evol. 2019:36: 500–515. https://doi.org/10.1093/molbev/msy246.
Frank SA, Patten MM. Sexual antagonism leads to a mosaic of X-autosome conflict. Evolution. 2020:74:495–498. https://doi.org/10.1111/evo.13918.
Fry JD. The genomic location of sexually antagonistic variation: some cautionary comments. Evolution. 2010:64:1510–1516. https://doi.org/10.1111/j.1558-5646.2009.00898.x.
Galtier N. Adaptive protein evolution in animals and the effective population size hypothesis. PLoS Genet. 2016:12:e1005774. https://doi.org/10.1371/journal.pgen.1005774.
Garrigan D, et al. Genome diversity and divergence in *Drosophila mauritiana*: multiple signatures of faster X evolution. Genome Biol Evol. 2014:6:2444–2458. https://doi.org/10.1093/gbe/evu198.
Gerstein AC, Cleathero LA, Mandegar MA, Otto SP. Haploids adapt faster than diploids across a range of environments. J Evol Biol. 2011:24:531–540. https://doi.org/10.1111/j.1420-9101.2010.02188.x.
Gerstein AC, Kuzmin A, Otto SP. Loss-of-heterozygosity facilitates passage through Haldane's sieve for *Saccharomyces cerevisiae* undergoing adaptation. Nat Commun. 2014:5:3819. https://doi.org/10.1038/ncomms4819.
Goldberg A, Günther T, Rosenberg NA, Jakobsson M. Ancient X chromosomes reveal contrasting sex bias in Neolithic and Bronze Age Eurasian migrations. Proc Natl Acad Sci U S A. 2017: 114:2657–2662. https://doi.org/10.1073/pnas.1616392114.
Grantham R. Amino acid difference formula to help explain protein evolution. Science. 1974:185:862–864. https://doi.org/10.1126/science.185.4154.862.
Grieshop K, et al. Expression divergence in response to sex-biased selection. Mol Biol Evol. 2025:42:msaf099. https://doi.org/10.1093/molbev/msaf099.
Haldane JBS. A mathematical theory of natural and artificial selection, part V: selection and mutation. Math Proc Camb Philos Soc. 1927:23:838–844. https://doi.org/10.1017/S0305004100015644.
Halligan DL, et al. Evidence for pervasive adaptive protein evolution in wild mice. PLoS Genet. 2010:6:e1000825. https://doi.org/10.1371/journal.pgen.1000825.
Hammer MF, et al. The ratio of human X chromosome to autosome diversity is positively correlated with genetic distance from genes. Nat Genet. 2010:42:830–831. https://doi.org/10.1038/ng.651.
Harr B, et al. Genomic resources for wild populations of the house mouse, *Mus musculus* and its close relative *Mus spretus*. Sci Data. 2016:3:160075. https://doi.org/10.1038/sdata.2016.75.
Harris M, Garud NR. Enrichment of hard sweeps on the X chromosome in *Drosophila melanogaster*. Mol Biol Evol. 2023:40: msac268. https://doi.org/10.1093/molbev/msac268.
Harris M, Kim BY, Garud N. Enrichment of hard sweeps on the X chromosome compared to autosomes in six *Drosophila* species. Genetics. 2024:226:iyae019. https://doi.org/10.1093/genetics/iyae019.
Hayes K, Barton HJ, Zeng K. A study of faster-Z evolution in the great tit (*Parus major*). Genome Biol Evol. 2020:12:210–222. https://doi.org/10.1093/gbe/evaa044.

Downloaded from academic.oup.com/gbe/article/18/10/evag259/8907347 by library@ist.ac.at user on 23 October 2026

Hayward LK, Sella G. Polygenic adaptation after a sudden change in environment. eLife. 2022:11:e66697. https://doi.org/10.7554/eLife.66697.
Huber CD, Kim BY, Lohmueller KE. Population genetic models of GERP scores suggest pervasive turnover of constrained sites across mammalian evolution. PLoS Genet. 2020:16:e1008827. https://doi.org/10.1371/journal.pgen.1008827.
Hvilsom C, et al. Extensive X-linked adaptive evolution in central chimpanzees. Proc Natl Acad Sci U S A. 2012:109:2054–2059. https://doi.org/10.1073/pnas.1106877109.
Jackson BC, et al. Variation in the intensity of selection on codon bias over time causes contrasting patterns of base composition evolution in *Drosophila*. Genome Biol Evol. 2017:9:102–123. https://doi.org/10.1093/gbe/evw291.
Jaquiéry J, et al. Disentangling the causes for faster-X evolution in aphids. Genome Biol Evol. 2018:10:507–520. https://doi.org/10.1093/gbe/evy015.
Juric I, Aeschbacher S, Coop G. The strength of selection against Neanderthal introgression. PLoS Genet. 2016:12:e1006340. https://doi.org/10.1371/journal.pgen.1006340.
Keightley PD, et al. Analysis of the genome sequences of three *Drosophila melanogaster* spontaneous mutation accumulation lines. Genome Res. 2009:19:1195–1201. https://doi.org/10.1101/gr.091231.109.
Keightley PD, Eyre-Walker A. Joint inference of the distribution of fitness effects of deleterious mutations and population demography based on nucleotide polymorphism frequencies. Genetics. 2007:177:2251–2261. https://doi.org/10.1534/genetics.107.080663.
Kong A, et al. Rate of de novo mutations and the importance of father's age to disease risk. Nature. 2012:488:471–475. https://doi.org/10.1038/nature11396.
Kousathanas A, Halligan DL, Keightley PD. Faster-X adaptive protein evolution in house mice. Genetics. 2014:196:1131–1143. https://doi.org/10.1534/genetics.113.158246.
Lack JB, et al. A thousand fly genomes: an expanded *Drosophila* genome Nexus. Mol Biol Evol. 2016:33:3308–3313. https://doi.org/10.1093/molbev/msw195.
Langergraber KE, et al. Generation times in wild chimpanzees and gorillas suggest earlier divergence times in great ape and human evolution. Proc Natl Acad Sci U S A. 2012:109:15716–15721. https://doi.org/10.1073/pnas.1211740109.
Lasne C, Sgrò CM, Connallon T. The relative contributions of the *X* chromosome and autosomes to local adaptation. Genetics. 2017:205:1285–1304. https://doi.org/10.1534/genetics.116.194670.
Leffler EM, et al. Revisiting an old riddle: what determines genetic diversity levels within species? PLoS Biol. 2012:10:e1001388. https://doi.org/10.1371/journal.pbio.1001388.
Leffler EM, et al. Multiple instances of ancient balancing selection shared between humans and chimpanzees. Science. 2013:339:1578–1582. https://doi.org/10.1126/science.1234070.
Lohmueller KE, Degenhardt JD, Keinan A. Sex-averaged recombination and mutation rates on the X chromosome: a comment on Labuda et al. Am J Hum Genet. 2010:86:978–980. https://doi.org/10.1016/j.ajhg.2010.03.021.
Lynch M, et al. The divergence of mutation rates and spectra across the tree of life. EMBO Rep. 2023:24:e57561. https://doi.org/10.15252/embr.202357561.
Mallet MA, Bouchard JM, Kimber CM, Chippindale AK. Experimental mutation-accumulation on the X chromosome of *Drosophila melanogaster* reveals stronger selection on males than females. BMC Evol Biol. 2011:11:156. https://doi.org/10.1186/1471-2148-11-156.
Mank JE, Vicoso B, Berlin S, Charlesworth B. Effective population size and the faster-X effect: empirical results and their interpretation. Evolution. 2010:64:663–674. https://doi.org/10.1111/j.1558-5646.2009.00853.x.
Manna F, Martin G, Lenormand T. Fitness landscapes: an alternative theory for the dominance of mutation. Genetics. 2011:189:923–937. https://doi.org/10.1534/genetics.111.132944.
Marad DA, Buskirk SW, Lang GI. Altered access to beneficial mutations slows adaptation and biases fixed mutations in diploids. Nat Ecol Evol. 2018:2:882–889. https://doi.org/10.1038/s41559-018-0503-9.
Martin R, Tate AT. Pleiotropy increases with gene age in six model multicellular eukaryotes. Evol Lett. 2025:9:589–597. https://doi.org/10.1093/evlett/qraf025.
Masly JP, Presgraves DC. High-resolution genome-wide dissection of the two rules of speciation in *Drosophila*. PLoS Biol. 2007:5:e243. https://doi.org/10.1371/journal.pbio.0050243.
McDonald JH, Kreitman M. Adaptive protein evolution at the Adh locus in *Drosophila*. Nature. 1991:351:652–654. https://doi.org/10.1038/351652a0.
McDonough Y, Connallon T. Effects of population size change on the genetics of adaptation following an abrupt change in environment. Evolution. 2023:77:1852–1863. https://doi.org/10.1093/evolut/qpad103.
McDonough Y, Ruzicka F, Connallon T. Reconciling theories of dominance with the relative rates of adaptive substitution on sex chromosomes and autosomes. Proc Natl Acad Sci U S A. 2024:121:e2406335121. https://doi.org/10.1073/pnas.2406335121.
Meisel RP, Connallon T. The faster-X effect: integrating theory and data. Trends Genet. 2013:29:537–544. https://doi.org/10.1016/j.tig.2013.05.009.
Meisel RP, Han MV, Hahn MW. A complex suite of forces drives gene traffic from *Drosophila* X chromosomes. Genome Biol Evol. 2009:1:176–188. https://doi.org/10.1093/gbe/evp018.
Ming MJ, Cheng C, Kirkpatrick M, Harpak A. No evidence for sex-differential transcriptomes driving genome-wide sex-differential natural selection. Am J Hum Genet. 2025:112:254–260. https://doi.org/10.1016/j.ajhg.2024.12.016.
Mirchandani CD, et al. A fast, reproducible, high-throughput variant calling workflow for population genomics. Mol Biol Evol. 2024:41:msad270. https://doi.org/10.1093/molbev/msad270.
Miyata T, et al. Male-driven molecular evolution: a model and nucleotide sequence analysis. Cold Spring Harb Symp Quant Biol. 1987:52:863–867. https://doi.org/10.1101/SQB.1987.052.01.094.
Mongue AJ, Baird RB. Genetic drift drives faster-Z evolution in the salmon louse *Lepeophtheirus salmonis*. Evolution. 2024:78:1594–1605. https://doi.org/10.1093/evolut/qpae090.
Mongue AJ, Hansen ME, Walters JR. Support for faster and more adaptive Z chromosome evolution in two divergent lepidopteran lineages*. Evolution. 2022:76:332–345. https://doi.org/10.1111/evo.14341.
Moutinho AF, Eyre-Walker A, Dutheil JY. Strong evidence for the adaptive walk model of gene evolution in *Drosophila* and *Arabidopsis*. PLoS Biol. 2022:20:e3001775. https://doi.org/10.1371/journal.pbio.3001775.
Mrnjavac A, Vicoso B. Reduced efficacy of selection on a young Z chromosome region of *Schistosoma japonicum*. Genome Biol Evol. 2025:17:evaf021. https://doi.org/10.1093/gbe/evaf021.
Muralidhar P, Coop G. Polygenic response of sex chromosomes to sexual antagonism. Evolution. 2023:78:539–554. https://doi.org/10.1093/evolut/qpad231.

Downloaded from academic.oup.com/gbe/article/18/10/evag259/8907347 by library@ist.ac.at user on 23 October 2026

Muralidhar P, Veller C. Dominance shifts increase the likelihood of soft selective sweeps. Evolution. 2022:76:966–984. https://doi.org/10.1111/evo.14459.
Ng PC, Henikoff S. Predicting deleterious amino acid substitutions. Genome Res. 2001:11:863–874. https://doi.org/10.1101/gr.176601.
Nocchi G, Whiting JR, Yeaman S. Repeated global adaptation across plant species. Proc Natl Acad Sci U S A. 2024:121:e2406832121. https://doi.org/10.1073/pnas.2406832121.
Obbard DJ, et al. Estimating divergence dates and substitution rates in the *Drosophila* phylogeny. Mol Biol Evol. 2012:29:3459–3473. https://doi.org/10.1093/molbev/mss150.
Orr HA. A test of Fisher's theory of dominance. Proc Natl Acad Sci U S A. 1991:88:11413–11415. https://doi.org/10.1073/pnas.88.24.11413.
Orr HA. The population genetics of adaptation: the distribution of factors fixed during adaptive evolution. Evolution. 1998:52:935–949. https://doi.org/10.1111/j.1558-5646.1998.tb01823.x.
Orr HA. The population genetics of beneficial mutations. Philos Trans R Soc B: Biol Sci. 2010:365:1195–1201. https://doi.org/10.1098/rstb.2009.0282.
Orr HA, Betancourt AJ. Haldane's sieve and adaptation from the standing genetic variation. Genetics. 2001:157:875–884. https://doi.org/10.1093/genetics/157.2.875.
Orr HA, Otto SP. Does diploidy increase the rate of adaptation? Genetics. 1994:136:1475–1480. https://doi.org/10.1093/genetics/136.4.1475.
Osada N, Matsudaira K, Hamada Y, Malaivijitnond S. Testing sex-biased admixture origin of macaque species using autosomal and X-chromosomal genomic sequences. Genome Biol Evol. 2020:13:evaa209. https://doi.org/10.1093/gbe/evaa209.
Padhy AA, et al. Systematic profiling of dominant ubiquitin variants reveals key functional nodes contributing to evolutionary selection. Cell Rep. 2023:42:113064. https://doi.org/10.1016/j.celrep.2023.113064.
Page AJ, et al. SNP-sites : rapid efficient extraction of SNPs from multi-FASTA alignments. Microb Genom. 2016:2:e000056. https://doi.org/10.1099/mgen.0.000056.
Pamilo P. Genic variation at sex-linked loci: quantification of regular selection models. Hereditas. 1979:91:129–133. https://doi.org/10.1111/j.1601-5223.1979.tb01652.x.
Pertea G, Pertea M. GFF utilities: GffRead and GffCompare. F1000Res. 2020:9:ISCB Comm J-304. https://doi.org/10.12688/f1000research.23297.2.
Pinharanda A, et al. Sexually dimorphic gene expression and transcriptome evolution provide mixed evidence for a fast-Z effect in *Heliconius*. J Evol Biol. 2019:32:194–204. https://doi.org/10.1111/jeb.13410.
Presgraves DC. Evaluating genomic signatures of "the large X-effect" during complex speciation. Mol Ecol. 2018:27:3822–3830. https://doi.org/10.1111/mec.14777.
Quinlan AR, Hall IM. BEDTools: a flexible suite of utilities for comparing genomic features. Bioinformatics. 2010:26:841–842. https://doi.org/10.1093/bioinformatics/btq033.
Ranwez V, Harispe S, Delsuc F, Douzery EJP. MACSE: multiple alignment of coding SEquences accounting for frameshifts and stop codons. PLoS One. 2011:6:e22594. https://doi.org/10.1371/journal.pone.0022594.
Rice WR. Sex chromosomes and the evolution of sexual dimorphism. Evolution. 1984:38:735–742. https://doi.org/10.2307/2408385.
Ronfort J, Glémin S. Mating system, Haldane's sieve, and the domestication process. Evolution. 2013:67:1518–1526. https://doi.org/10.1111/evo.12025.
Rousselle M, et al. Hemizygosity enhances purifying selection: lack of fast-Z evolution in two satyrine butterflies. Genome Biol Evol. 2016:8:3108–3119. https://doi.org/10.1093/gbe/evw214.
Rousselle M, et al. Influence of recombination and GC-biased gene conversion on the adaptive and nonadaptive substitution rate in mammals versus birds. Mol Biol Evol. 2019:36:458–471. https://doi.org/10.1093/molbev/msy243.
Rousselle M, et al. Is adaptation limited by mutation? A timescale-dependent effect of genetic diversity on the adaptive substitution rate in animals. PLoS Genet. 2020:16:e1008668. https://doi.org/10.1371/journal.pgen.1008668.
RStudio Team. 2020. RStudio: Integrated development environment for R. RStudio, PBC. http://www.rstudio.com/
Ruzicka F, et al. Genome-wide sexually antagonistic variants reveal long-standing constraints on sexual dimorphism in fruit flies. PLoS Biol. 2019:17:e3000244. https://doi.org/10.1371/journal.pbio.3000244.
Ruzicka F, et al. A century of theories of balancing selection. Biol Rev Camb Philos Soc. 2026:101:804–825. https://doi.org/10.1111/brv.70103.
Ruzicka F, Connallon T. Is the X chromosome a hot spot for sexually antagonistic polymorphisms? Biases in current empirical tests of classical theory. Proc R Soc Lond B Biol Sci. 2020:287:20201869. https://doi.org/10.1098/rspb.2020.1869.
Ruzicka F, Connallon T. An unbiased test reveals no enrichment of sexually antagonistic polymorphisms on the human X chromosome. Proc R Soc Lond B Biol Sci. 2022:289:20212314. https://doi.org/10.1098/rspb.2021.2314.
Ruzicka F, Connallon T, Reuter M. Sex differences in deleterious mutational effects in *Drosophila melanogaster*: combining quantitative and population genetic insights. Genetics. 2021:219:iyab143. https://doi.org/10.1093/genetics/iyab143.
Sackton TB, et al. Positive selection drives faster-Z evolution in silkmoths. Evolution. 2014:68:2331–2342. https://doi.org/10.1111/evo.12449.
Sankararaman S, Mallick S, Patterson N, Reich D. The combined landscape of Denisovan and Neanderthal ancestry in present-day humans. Curr Biol. 2016:26:1241–1247. https://doi.org/10.1016/j.cub.2016.03.037.
Sellis D, et al. Heterozygote advantage is a common outcome of adaptation in *Saccharomyces cerevisiae*. Genetics. 2016:203:1401–1413. https://doi.org/10.1534/genetics.115.185165.
Sellis D, Callahan BJ, Petrov DA, Messer PW. Heterozygote advantage as a natural consequence of adaptation in diploids. Proc Natl Acad Sci U S A. 2011:108:20666–20671. https://doi.org/10.1073/pnas.1114573108.
Sidorenko J, et al. The effect of X-linked dosage compensation on complex trait variation. Nat Commun. 2019:10:3009. https://doi.org/10.1038/s41467-019-10598-y.
Simmons MJ, Crow JF. Mutations affecting fitness in *Drosophila* populations. Annu Rev Genet. 1977:11:49–78. https://doi.org/10.1146/annurev.ge.11.120177.000405.
Singh ND, Larracuente AM, Clark AG. Contrasting the efficacy of selection on the X and autosomes in *Drosophila*. Mol Biol Evol. 2008:25:454–467. https://doi.org/10.1093/molbev/msm275.
Smith NGC, Eyre-Walker A. Adaptive protein evolution in *Drosophila*. Nature. 2002:415:1022–1024. https://doi.org/10.1038/4151022a.
Soni V, Vos M, Eyre-Walker A. A new test suggests hundreds of amino acid polymorphisms in humans are subject to balancing selection. PLoS Biol. 2022:20:e3001645. https://doi.org/10.1371/journal.pbio.3001645.
Sultanova Z, Andic M, Carazo P. The "unguarded-X" and the genetic architecture of lifespan: inbreeding results in a potentially

Downloaded from academic.oup.com/gbe/article/18/10/evag259/8907347 by library@ist.ac.at user on 23 October 2026

maladaptive sex-specific reduction of female lifespan in *Drosophila melanogaster*. Evolution. 2018:72:540–552. https://doi.org/10.1111/evo.13426.
Sultanova Z, Downing PA, Carazo P. Genetic sex determination, sex chromosome size and sex-specific lifespans across tetrapods. J Evol Biol. 2023:36:480–494. https://doi.org/10.1111/jeb.14130.
Suvorov A, et al. Widespread introgression across a phylogeny of 155 *Drosophila* genomes. Curr Biol. 2022:32:111–123.e5. https://doi.org/10.1016/j.cub.2021.10.052.
Suzuki H, et al. Temporal, spatial, and ecological modes of evolution of Eurasian *Mus* based on mitochondrial and nuclear gene sequences. Mol Phylogenet Evol. 2004:33:626–646. https://doi.org/10.1016/j.ympev.2004.08.003.
The 1000 Genomes Project Consortium. A global reference for human genetic variation. Nature. 2015:526:68–74. https://doi.org/10.1038/nature15393.
Thybert D, et al. Repeat associated mechanisms of genome evolution and function revealed by the *Mus caroli* and *Mus pahari* genomes. Genome Res. 2018:28:448–459. https://doi.org/10.1101/gr.234096.117.
Toups MA, Hahn MW. Retrogenes reveal the direction of sex-chromosome evolution in mosquitoes. Genetics. 2010:186:763–766. https://doi.org/10.1534/genetics.110.118794.
Turelli M, Orr HA. The dominance theory of Haldane's rule. Genetics. 1995:140:389–402. https://doi.org/10.1093/genetics/140.1.389.
Turelli M, Orr HA. Dominance, epistasis and the genetics of postzygotic isolation. Genetics. 2000:154:1663–1679. https://doi.org/10.1093/genetics/154.4.1663.
Vaser R, et al. SIFT missense predictions for genomes. Nat Protoc. 2016:11:1–9. https://doi.org/10.1038/nprot.2015.123.
Veeramah KR, et al. Evidence for increased levels of positive and negative selection on the X chromosome versus autosomes in humans. Mol Biol Evol. 2014:31:2267–2282. https://doi.org/10.1093/molbev/msu166.
Vibranovski MD, Zhang Y, Long M. General gene movement off the X chromosome in the *Drosophila* genus. Genome Res. 2009:19:897–903. https://doi.org/10.1101/gr.088609.108.
Vicoso B, et al. Comparative sex chromosome genomics in snakes: differentiation, evolutionary strata, and lack of global dosage compensation. PLoS Biol. 2013:11:e1001643. https://doi.org/10.1371/journal.pbio.1001643.
Vicoso B, Charlesworth B. Evolution on the X chromosome: unusual patterns and processes. Nat Rev Genet. 2006:7:645–653. https://doi.org/10.1038/nrg1914.
Vicoso B, Charlesworth B. Effective population size and the faster-X effect: an extended model. Evolution. 2009:63:2413–2426. https://doi.org/10.1111/j.1558-5646.2009.00719.x.
Vicoso B, Haddrill PR, Charlesworth B. A multispecies approach for comparing sequence evolution of X-linked and autosomal sites in *Drosophila*. Genet Res (Camb). 2008:90:421–431. https://doi.org/10.1017/S0016672308009804.
Waxman D, Welch JJ. Fisher's microscope and Haldane's ellipse. Am Nat. 2005:166:447–457. https://doi.org/10.1086/444404.
Wilson Sayres MA. Genetic diversity on the sex chromosomes. Genome Biol Evol. 2018:10:1064–1078. https://doi.org/10.1093/gbe/evy039.
Wilson Sayres MA, Makova KD. Genome analyses substantiate male mutation bias in many species. BioEssays. 2011:33:938–945. https://doi.org/10.1002/bies.201100091.
Wright AE, et al. Variation in promiscuity and sexual selection drives avian rate of faster-Z evolution. Mol Ecol. 2015:24:1218–1235. https://doi.org/10.1111/mec.13113.
Zeyl C, Vanderford T, Carter M. An evolutionary advantage of haploidy in large yeast populations. Science. 2003:299:555–558. https://doi.org/10.1126/science.1078417.

Associate editor: Charles Baer

Downloaded from academic.oup.com/gbe/article/18/10/evag259/8907347 by library@ist.ac.at user on 23 October 2026